IEEE Access
Multidisciplinary | Rapid Review | Open Access Journal

Received June 6, 2019, accepted June 13, 2019, date of publication June 19, 2019, date of current version July 8, 2019.

Digital Object Identifier 10.1109/ACCESS.2019.2923654

A Loop Pairing Method for Multivariable Control Systems Under a Multi-Objective Optimization Approach

VÍCTOR HUILCAPI[1], XAVIER BLASCO[2], JUAN MANUEL HERRERO[2], AND GILBERTO REYNOSO-MEZA[3]

[1]Facultad de Ingenierías, Universidad Politécnica Salesiana, Guayaquil 09014752, Ecuador
[2]Instituto Universitario de Automática e Informática Industrial, Universitat Politècnica de València, 46022 Valencia, Spain
[3]Programa de Pós-Graduação em Engenharia de Produção e Sistemas (PPGEPS), Pontifícia Universidade Católica do Paraná (PUCPR), Curitiba 80215-901, Brazil

Corresponding author: Víctor Huilcapi (vhuilcapi@ups.edu.ec)

This work was supported in part by the Ministerio de Economía y Competitividad, Spain, under Grant DPI2015-71443-R, in part by the National Council of Scientific and Technological Development of Brazil (CNPq) under Grant PQ2/304066/2016-8 and Grant UN/437105/2018-0.t, and in part by the Universidad Politécnica Salesiana, Ecuador, under Grant CB-755-2015.

ABSTRACT This paper proposes a new method for the selection of input–output pairing in decentralized control structures for multivariable systems. This method proposes the input–output pairing problem as a multi-objective optimization problem (MOP). For each control structure and loop pairing analyzed, a different design concept is proposed and a MOP is stated. All MOPs share the same design objectives, and Pareto fronts associated with each design concept can be compared globally under a multi-objective (MO) approach. The design objectives were chosen for the MOP, as well as the designer's preferences, have an important role in selecting a certain loop pairing. The main contribution of the proposed approach is that it enables a systematic analysis of the conflicts between the objectives and the performance of a control system. The method enables selecting a certain input–output pairing and a suitable tuning of the controller directly using information that a designer can interpret. To show the application of the methodology, two loop pairing examples are presented, one of them for a two-input–output system (with four scenarios of analysis), and the other for a three-input–output system (with one scenario of analysis). Through the examples presented in this paper, it is evident how the designer can affect the loop pairing to be used, either by choosing the objectives or preferences.

INDEX TERMS Multivariable control system, input-output pairing, decentralized control structures, multi-objective evolutionary optimization, Pareto front.

I. INTRODUCTION

The development and application of control strategies for systems with multiple-inputs and multiple-outputs (MIMO) is a topic of great interest. The complexity of the systems has increased over time and it is now a challenge to control multivariable systems. To propose a solution to the problem of controlling complex MIMO systems, two major approaches have been proposed: centralized control and decentralized control structures [1]– [3]. Although each approach has advantages and disadvantages, in recent years applications with decentralized control structures have increased in number because of the ease of implementation and maintenance. Decentralized control structures also behave robustly in the face of fault and model uncertainties [4]– [7].

The efficiency of the decentralized control structures in the MIMO systems largely depends on the adequate selection of the input-output pairing. For a MIMO system with n inputs and n outputs, there are $n!$ possible input-output pairings that enable system control. Some of the main methods for the selection of input-output pairings are shown in [8]. The problem of how to select input-output pairings in linear multivariable plants, was treated several decades ago with the relative gain array (RGA) method. RGA simply uses the static gains matrix (zero frequency) of the system [9]. Since the RGA method became available, several extensions have been

The associate editor coordinating the review of this manuscript and approving it for publication was Xiaosong Hu.

This work is licensed under a Creative Commons Attribution 3.0 License. For more information, see http://creativecommons.org/licenses/by/3.0/

proposed to adapt it to other scenarios and requirements. For example, for MIMO systems with differing numbers of inputs and outputs, the nonsquare relative gain array (NSRGA) was defined [10]. The dynamic relative gain array (DRGA) considers the dynamics of the system and generalizes the application of RGA to non-zero frequencies [11]. Another proposed approach known as partial relative gains (PRG) [12] proposes a version of the RGA method that considers partially controlled systems and its use is recommended when RGA fails or is ambiguous. The effective relative gain array (ERGA) method was introduced to quantify the interaction between the control loops of a MIMO system. The ERGA method defines an energy transmission relation to achieve a minimum interaction within the frequency range of interest [13]. The absolute relative gains array (ARGA) was proposed to solve integrity and robustness problems due to the variation of parameters and effects of non-linearities in multivariable systems [14]. To analyze the interactions of the control loops of multivariable systems in permanent and transitory regimes, the relative normalized gain array (RNGA) was proposed [15]. Other works that propose methodologies to face the complex problem of finding optimal input-output pairings for the control of MIMO systems are shown in [16]– [19].

After the conventional input-output pairing methods, other approaches have emerged. For example, in [20] a technique based on the effective open-loop transfer function (EOTF) that enables the decomposition of the MIMO system into n independent systems of a single input-output (SISO) was proposed. Some methods use artificial intelligence techniques [21], [22], and others are based on the passivity theory [23], [24]. From another point of view, methods for the selection of input-output pairings in decentralized control systems can involve an optimization process ,which can be multi-objective as in [25]– [27].

It should be noted that the stated methods can suggest different types of input-output pairings for the same MIMO system, and the designer's preferences and system requirements define the selection of one or another loop pairing. Additionally, the control structure and the adjustment of its parameters have an important role in the performance obtained from the system. This may condition the selection of the input-output pairing, as noted in [12] and shown in [26], where a bi-objective optimization approach is presented to choose a loop pairing in a 2×2 MIMO system.

Following the approach presented in [26], this article aims to contribute to the generation of a framework that enables the selection of input-output pairings more in accordance with the needs and preferences of the control engineer. An m-dimensional multi-objective optimization approach to incorporating differing design objectives to be satisfied is used. In addition, each proposed multivariable control structure (this entails a certain loop pairing and type of control) assumes a different design concept. The optimization process associated with the parameter adjustment of a controller generates a Pareto front. Therefore, it is necessary to establish an adequate procedure that allows comparing the various design concepts (with their corresponding Pareto fronts) that are generated.

Evolutionary multi-objective algorithms (MOEAs) have been used successfully in controller tuning due to their flexibility to optimize non-convex functions and to handle constraints [28]– [31].

An MOEA is responsible for characterizing the Pareto front and later the decision maker (DM) selects the final solution based on his/her preferences. Some methodologies and tools have been developed to help the DM in the task of selecting optimal solutions [33], [34]. The visualization tools for the Pareto front are widely accepted and constitute an effective technique for the analysis and selection of solutions from this front [35], [36]. The visualization of the Pareto front is relatively simple for a bi-dimensional MOP [37], [38], but if the number of objectives is greater, graphic analysis becomes more complicated and requires alternative tools. The level diagrams (LD) tool features interesting characteristics: it is easy to interpret the results; it is flexible enough to incorporate various points of view (using the change of synchronization norm); it offers coloring and highlighting solutions; interactivity; and the ability to compare design concepts. All the features of the LD tool are desirable for Pareto front visualization [39]– [41].

In this paper the ev-MOGA algorithm[1] [32] is used for the characterization of the Pareto fronts associated with each design concept and the level diagrams tool[2] for the comparison of the fronts using as a norm the QI indicator proposed in [42]. LD and the quality indicator QI enable the global comparison of Pareto fronts using a dominance analysis. It is important to mention that the MOEA used does not condition the proposed methodology, and therefore, this article is not intended to make a performance comparison with other MOEAs. Although ev-MOGA is the chosen MOEA, similar results would have been obtained with other MOEAs.

The proposed multi-objective approach is applied to two systems (a 2×2 system and a 3×3 system) with the aim of selecting the input-output pairing and, simultaneously, the most appropriate parameter tuning of the control system, according to the preferences of the designer. For the 2×2 system (which is taken as a base example in order to present the possibilities of the proposed methodology), four analysis scenarios are proposed: scenario 1 with MOPs of two objectives, scenario 2 and 4 with MOPs of four objectives and scenario 3 with MOPs of eight objectives. In the first three scenarios, the same objectives are used to evaluate the performance of the controlled system and the design objectives are increasingly disaggregated to obtain more

[1] *ev*-MOGA algorithm available at: https://es.mathworks.com/matlabcentral/fileexchange/31080-ev-moga-multiobjective-evolutionary-algorithm.

[2] Level diagrams interactive tool available at: https://es.mathworks.com/matlabcentral/fileexchange/62224-interactive-tool-for-decision-making-in-multiobjective-optimization-with-level-diagrams.

information about the compensation that occurs between them. It is observed that for an appropriate loop pairing selection, the aggregation of objectives can hide relevant information. In the fourth scenario, other objectives are proposed to show how the preferences of the designer can influence the loop pairing choice. In the 3 × 3 system, a scenario with six design objectives is set, in order to analyze the compensation between the errors of each output and the control efforts of each input individually. This example is intended to show the scalability of the methodology, which is applicable to systems of any number of inputs-outputs. Obviously, the increase in 1) the number of inputs-outputs, 2) the number of alternative loop pairings to be studied and 3) the complexity of the simulations associated with the selected objectives, increases the computational cost and makes the analysis phase more difficult.

This paper examines the proposals in [11] and [15], where each proposed methodology suggests different types of loop pairings, as well as the proposal in [26].

Through the examples presented, the ability of the proposed methodology to offer a control engineer a multi-dimensional framework to select optimal input-output pairings is demonstrated. The selection of a loop pairing depends on a designer's preferences. Constraints on design objectives are taken into account in each MOP in order to avoid solutions with low performance.

This paper is organized as follows: Section II details the basics of multi-objective optimization and an introductory explanation about comparison of design concepts. Section III shows a new framework for selecting input-output pairings in MIMO systems with the proposed multi-objective approach. In sections IV and V the proposed methodology is applied to 2 × 2 and 3 × 3 systems with several analysis scenarios. Finally some conclusions are presented in Section VI. Appendix A presents an analysis of the computational cost of the proposed methodology.

II. THEORETICAL CONSIDERATIONS OF MULTI-OBJECTIVE OPTIMIZATION

Engineering problems usually require handling situations where multiple objectives need to be optimized simultaneously, and this action often presents some type of conflict (improving some objectives worsens others). Multi-objective optimization techniques deal with these problems. A multi-objective optimization problem (MOP) can be stated as in (1)-(5).

$$\min_{\mathbf{x}\in \mathrm{D}} \mathbf{J}(\mathbf{x}) \tag{1}$$

$$\mathbf{J}(\mathbf{x}) = \{J_1(\mathbf{x}), J_2(\mathbf{x}), \ldots, J_s(\mathbf{x})\} \tag{2}$$

$$\text{subject to: } g(\mathbf{x}) \leq 0 \tag{3}$$

$$h(\mathbf{x}) = 0 \tag{4}$$

$$\underline{\mathbf{x}} \leq \mathbf{x}_i \leq \overline{\mathbf{x}}, i = [1, \ldots, n] \tag{5}$$

where $\mathbf{x} = (x_1, x_2, \ldots x_n) \in \mathbf{R}^n$ is the decision vector; D is the decision space; $\mathbf{J}(\mathbf{x}) \in \mathbf{R}^m$ is the objective vector; $g(\mathbf{x})$, $h(\mathbf{x})$ are the constraint vectors; and $\underline{\mathbf{x}}$, $\overline{\mathbf{x}}$ are the upper and lower bounds of the decision space. In general, there is not a single optimal solution, but a set of optimal solutions with different trade-offs between design objectives, where no one is better than another. This set of Pareto optimal solutions is known as the Pareto front [43].

The Pareto optimal set $\mathbf{X}_p$, is based on the definition of Pareto dominance [44], and is formed by solutions that are not dominated by others. It is established that one vector $\mathbf{x}^1$ dominates another vector $\mathbf{x}^2$, (denoted by $\mathbf{x}^1 \preceq \mathbf{x}^2$), if $\mathbf{J}(\mathbf{x}^1)$ is not worse than $\mathbf{J}(\mathbf{x}^2)$ in all the objectives, and it is better in at least one objective (see Fig. 1). Pareto dominance is defined as in (6) and the Pareto optimal set $\mathbf{X}_p$ is defined as in (7)-(8).

$$\forall i \in \{1, \ldots, s\},\ \mathbf{J}_i(\mathbf{x}^1) \leq \mathbf{J}_i(\mathbf{x}^2) \wedge \exists \mathrm{k} \in \{1, \ldots, s\} : \mathbf{J}_{\mathrm{k}}(\mathbf{x}^1) < \mathbf{J}_{\mathrm{k}}(\mathbf{x}^2) \tag{6}$$

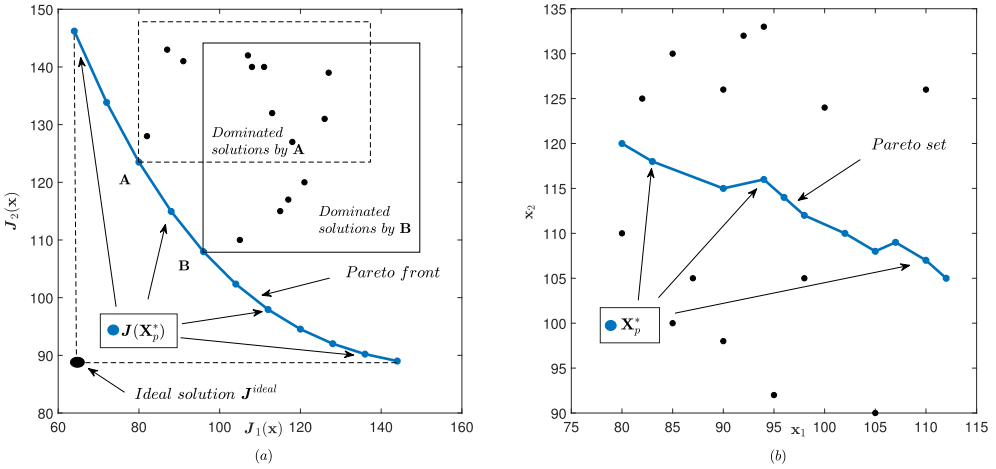

FIGURE 1. Pareto front, Pareto set and basic notion of Pareto dominance. (a) Pareto front for a bi-objective MOP. (b) Decision variables of the Pareto set.

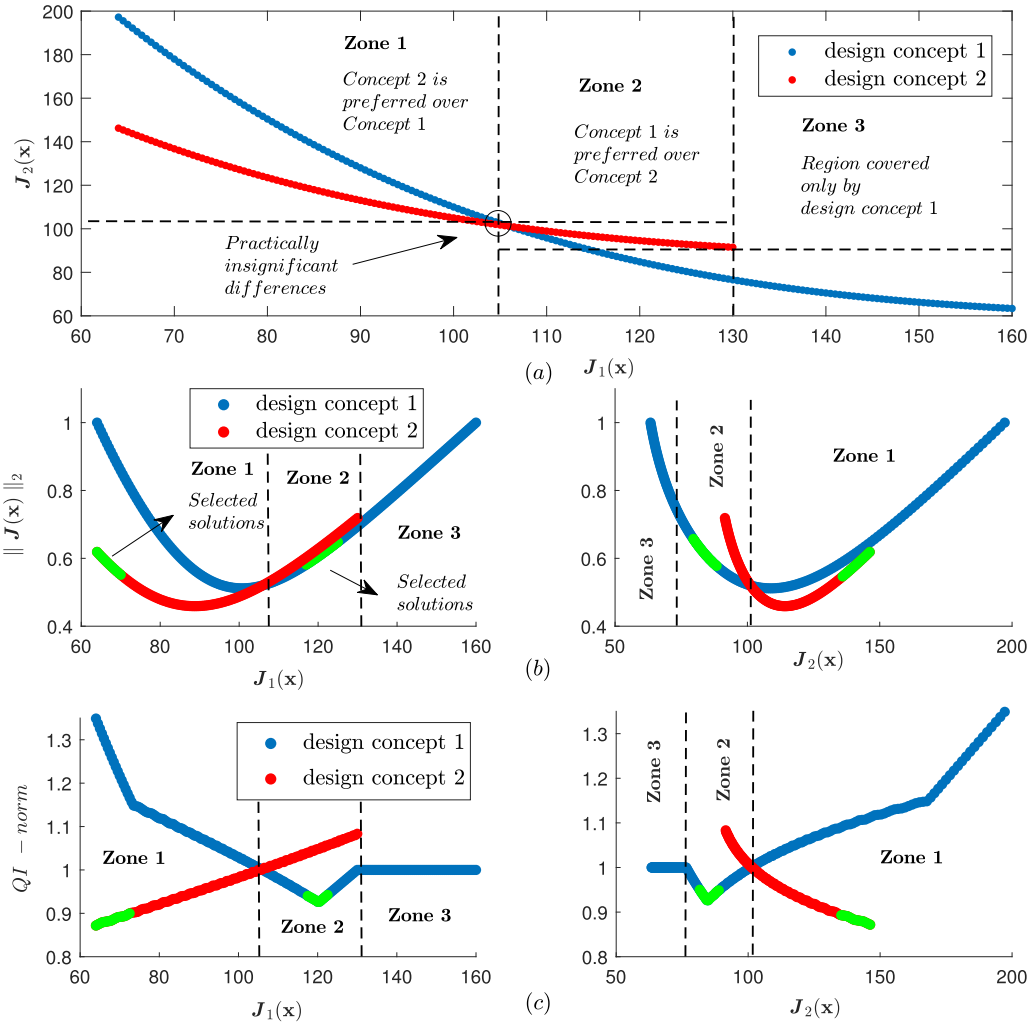

FIGURE 2. Pareto fronts and comparison of design concepts using *level diagrams* (LD). (a) Pareto fronts and zones of preference for design concepts 1 and 2. (b) Pareto fronts of design concepts 1 and 2 using LD with 2-norm. (c) Pareto fronts of design concepts 1 and 2 using LD with QI-norm.

$$\mathbf{X}_p = \{\mathbf{x} \in D | \nexists \mathbf{x}' \in D : \mathbf{x}' \leq \mathbf{x}\} \quad (7)$$

$$\mathbf{J}(\mathbf{X}_p) = \{\mathbf{J}(\mathbf{x}) | \mathbf{x} \in \mathbf{X}_p\} \quad (8)$$

In practice, optimization algorithms find a set of solutions $\mathbf{X}_p^* \subset \mathbf{X}_p$, and $\mathbf{J}(\mathbf{X}_p^*)$ represents $\mathbf{J}(\mathbf{X}_p)$ satisfactorily. Considering the set $\mathbf{X}_p^*$, a designer can select from it a solution according to his/her preferences or design specifications. For example, by selecting the solution that is closest (measured by some norm $||\quad||_n$) to the ideal point $\mathbf{J}^{ideal}$, which minimizes each objective of the MOP.

A preliminary notion to differentiate the strengths and weaknesses of the Pareto fronts when they are compared is proposed in [45]. In this work, a design concept is defined as an idea to solve a specific problem. For each design concept, an MOP is proposed, from which its Pareto front is obtained. In the context of process control, a design concept may be related to a particular control structure, or a certain input-output pairing, as proposed in [42]. In Fig. 2 the comparison of two design concepts in a bi-objective MOP using the level diagrams (LD) tool with different synchronizations (2-norm and QI-norm [42]) is shown. Three zones can be observed, each establishing a preference relation of one concept over another. In each zone of the Pareto fronts it is feasible to select solutions that correspond to different design alternatives that a designer can choose. In zone 1, design concept 2 dominates concept 1, and this is also observable in the LD, where the QI indicator of concept 2 is less than one ($QI < 1$) as shown in Fig. 2 (c). In zone 2, the opposite to zone 1 occurs, and zone 3 is only covered by design concept 1.

III. MULTI-OBJECTIVE PROPOSAL FOR THE SELECTION OF INPUT-OUTPUT PAIRINGS IN MULTIVARIABLE SYSTEMS

Consider a multivariable process to be controlled with n inputs $(u_1, \ldots, u_n)$ and n outputs $(y_1, \ldots, y_n)$ defined by a matrix of transfer functions according to equations (9), (10). The decentralized multivariable control of the process described in (9) is defined by: 1) a vector $\mathbf{c}_k$ that contains the controllers of each output (see equation 11 and 2) a loop pairing matrix $L_p^{c_k}$ which connects the outputs of the

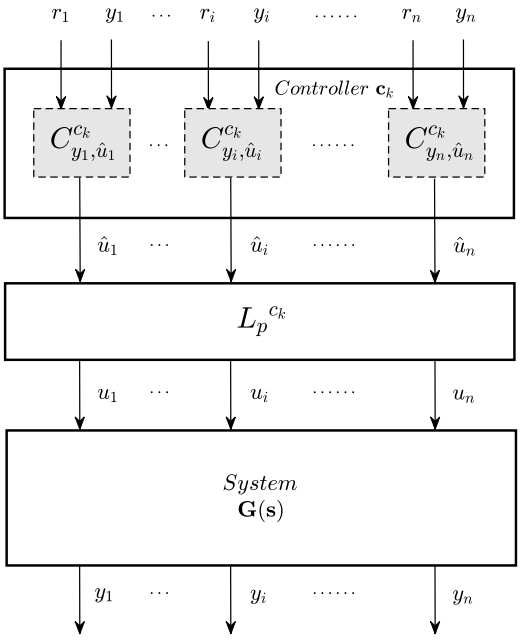

FIGURE 3. Block diagram of the decentralized multivariable control system defined in (11) and (12).

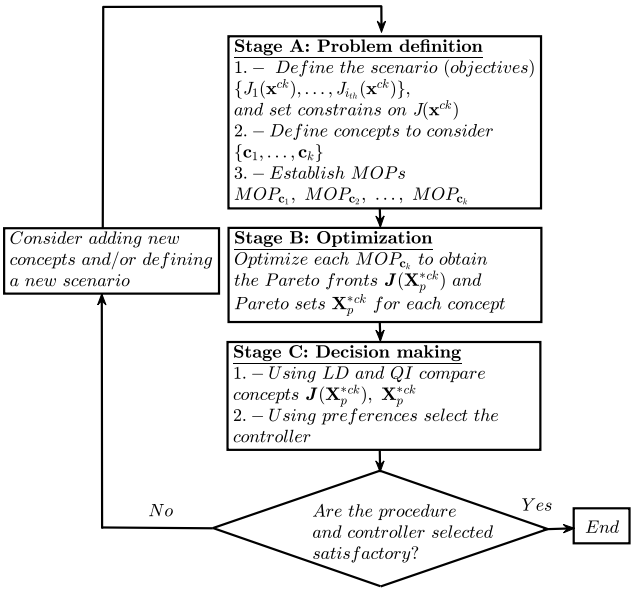

FIGURE 4. Flow chart of the proposed methodology for selecting pairings in multivariable systems.

controllers with the process inputs in order to establish a particular loop pairing (see equation 12).

$$\mathbf{Y(s)} = \mathbf{G(s)U(s)} \tag{9}$$

$$\begin{bmatrix} y_1(s) \\ \vdots \\ y_i(s) \\ \vdots \\ y_n(s) \end{bmatrix} = \begin{bmatrix} g_{11}(s) & g_{12}(s) & \dots & g_{1n}(s) \\ \vdots & \vdots & \dots & \vdots \\ g_{i1}(s) & g_{i2}(s) & \dots & g_{in}(s) \\ \vdots & \vdots & \dots & \vdots \\ g_{n1}(s) & g_{n2}(s) & \dots & g_{nn}(s) \end{bmatrix} \begin{bmatrix} u_1(s) \\ \vdots \\ u_i(s) \\ \vdots \\ u_n(s) \end{bmatrix} \tag{10}$$

$$\mathbf{c}_k = \left[C^{c_k}_{y_1,\hat{u}_1}, \dots C^{c_k}_{y_i,\hat{u}_i}, \dots, C^{c_k}_{y_n,\hat{u}_n} \right] \tag{11}$$

$$\begin{bmatrix} u_1(s) \\ \vdots \\ u_i(s) \\ \vdots \\ u_n(s) \end{bmatrix} = L_p^{c_k} \begin{bmatrix} \hat{u}_1(s) \\ \vdots \\ \hat{u}_i(s) \\ \vdots \\ \hat{u}_n(s) \end{bmatrix} \tag{12}$$

$$k \in \{1, \dots, w\};$$

where $C^{c_k}_{y_i,\hat{u}_i}$ represents the controller of the output y_i of the control $\mathbf{c}_k$. The controller $C^{c_k}_{y_i,\hat{u}_i}$ produces the control action $\hat{u}_i$, which is connected to one process input (u_i) by means of the loop pairing matrix $L_p^{c_k}$ (see Fig. 3). $L_p^{c_k}$ is a $n \times n$ Boolean matrix,

$$L_p^{c_k} = \begin{bmatrix} l_{11} & \dots & l_{1n} \\ \vdots & \dots & \vdots \\ l_{n1} & \dots & l_{nn} \end{bmatrix} \quad l_{ij} \in [0, 1] \quad \forall i, j \in [1 \dots n], \tag{13}$$

which contains only one "1" in each row and column, that is $\sum_{i=1}^{n} l_{ij} = 1 \ \forall j \in [1 \dots n]$ and $\sum_{j=1}^{n} l_{ij} = 1 \ \forall i \in [1 \dots n]$.

For example, in a 3×3 system where y_1 is controlled with u_2 ($l_{21} = 1$), y_2 is controlled with u_3 ($l_{32} = 1$) and y_3 is controlled with u_1 ($l_{13} = 1$), $L_p^{c_k}$ matrix would be the following:

$$L_p^{c_k} = \begin{bmatrix} 0 & 0 & 1 \\ 1 & 0 & 0 \\ 0 & 1 & 0 \end{bmatrix}.$$

Each controller $C^{c_k}_{y_i,\hat{u}_i}$ presents a vector of adjustment parameters $\mathbf{x}^{ck}_{yi}$, therefore the control of the process would be parameterized by the vector (14).

$$\mathbf{x}^{ck} = [\mathbf{x}^{ck}_{y1}, \dots, \mathbf{x}^{ck}_{yn}] \tag{14}$$

Each process control $\mathbf{c}_k$ represents an alternative or *design concept* to be optimally adjusted (through its parameters $\mathbf{x}^{ck}$ and a given loop pairing $L_p^{c_k}$). Since the optimization approach is multi-objective, each concept will generate a set of optimal Pareto solutions $\mathbf{X}^{ck}$ and its front $\mathbf{J}(\mathbf{X}^{ck})$.Therefore, for each design concept the MOP is proposed as in (15)-(17).

$$\mathbf{X}^{ck} = arg \min_{\mathbf{x}^{ck}} \mathbf{J}(\mathbf{x}^{ck}) \tag{15}$$

$$\mathbf{J}(\mathbf{x}^{ck}) = [J_1(\mathbf{x}^{ck}), \dots, J_s(\mathbf{x}^{ck})] \tag{16}$$

$$\underline{\mathbf{x}}^{ck} \leq \mathbf{x}^{ck} \leq \overline{\mathbf{x}}^{ck} \tag{17}$$

where, $\underline{\mathbf{x}}^{ck}$ and $\overline{\mathbf{x}}^{ck}$ are the lower and upper bounds of the design parameters $\mathbf{x}^{ck}$ of the concept $\mathbf{c}_k$, which define the search space. $J_1, \dots, J_s$ are the objectives to be minimized, and these objectives in the k optimization problems are associated with each design concept $\mathbf{c}_k$.

The proposed methodology is summarized in Fig. 4. In stage A, the k MOPs associated with the k concepts (the loop pairings and chosen control structures) are defined so

that the scenario (the design objectives) are used to compare them. In stage B, an optimization process is performed for each MOP and its Pareto fronts are obtained. In stage C, the Pareto fronts associated with each concept are compared using the LD and QI tools. Finally, the designer uses his/her preferences to choose a controller for the plant (the loop pairing and parameters of the controllers for each output). If the designer is not satisfied with the results of the established problem, the process establishing new concepts and/or different scenarios is repeated.

Some considerations about the computational cost of the proposal are presented in appendix A.

IV. EXAMPLE 1

To show the proposed multi-objective approach to select input-output pairings in MIMO systems, the example proposed in [11] is analyzed. For the process described in (18), RGA (Λ) suggests a diagonal pairing, and DRGA (Λ_D) suggests an off-diagonal pairing according to equation (19).

$$\begin{bmatrix} y_1(s) \\ y_2(s) \end{bmatrix} = \mathbf{G(s)} \begin{bmatrix} u_1(s) \\ u_2(s) \end{bmatrix} = \begin{bmatrix} \dfrac{5e^{-40s}}{100s+1} & \dfrac{1e^{-4s}}{10s+1} \\ \dfrac{-5e^{-4s}}{10s+1} & \dfrac{5e^{-40s}}{100s+1} \end{bmatrix} \begin{bmatrix} u_1(s) \\ u_2(s) \end{bmatrix} \tag{18}$$

$$\Lambda = \begin{bmatrix} \mathbf{0.8333} & 0.1667 \\ 0.1667 & \mathbf{0.8333} \end{bmatrix}; \Lambda_D = \begin{bmatrix} 0.25 & \mathbf{0.75} \\ \mathbf{0.75} & 0.25 \end{bmatrix} \tag{19}$$

To control the system, 1-DOF PIs controllers were designed and tuned by optimizing a single specific index or control objective. This index is also used for the determination of the most suitable input-output pairings between two alternatives or design concepts. The design concepts are: concept $\mathbf{c}_1$ or diagonal pairing; and concept $\mathbf{c}_2$ or off-diagonal pairing as shown in (20), (21) and (24),, (25) respectively. The controllers are shown in (22), (23) and (26), (27).

$$\mathbf{c}_1 = \left[C^{c_1}_{y_1,\hat{u}_1}, C^{c_1}_{y_2,\hat{u}_2} \right] \tag{20}$$

$$L^{c_1}_p = \begin{bmatrix} 1 & 0 \\ 0 & 1 \end{bmatrix} \tag{21}$$

$$C^{c_1}_{y_1,\hat{u}_1} = \frac{K_1^{c1}(s+1/Ti_1^{c1})}{s}, C^{c_1}_{y_2,\hat{u}_2} = \frac{K_2^{c1}(s+1/Ti_2^{c1})}{s} \tag{22}$$

$$\mathbf{x}^{c1} = \left[K_1^{c1}, Ti_1^{c1}, K_2^{c1}, Ti_2^{c1} \right] \tag{23}$$

$$\mathbf{c}_2 = \left[C^{c_2}_{y_1,\hat{u}_1}, C^{c_2}_{y_2,\hat{u}_2} \right] \tag{24}$$

$$L^{c_2}_p = \begin{bmatrix} 0 & 1 \\ 1 & 0 \end{bmatrix} \tag{25}$$

$$C^{c_2}_{y_1,\hat{u}_1} = \frac{K_1^{c2}(s+1/Ti_1^{c2})}{s}, C^{c_2}_{y_2,\hat{u}_2} = \frac{K_2^{c2}(s+1/Ti_2^{c2})}{s} \tag{26}$$

$$\mathbf{x}^{c2} = \left[K_1^{c2}, Ti_1^{c2}, K_2^{c2}, Ti_2^{c2} \right] \tag{27}$$

The authors propose in [11] to obtain the most adequate loop pairing by analyzing the $\mathbf{x}^{*c1}$ and $\mathbf{x}^{*c2}$ controllers. The $\mathbf{x}^{*c1}$ and $\mathbf{x}^{*c2}$ controllers are obtained from the optimization of a single objective that agglutinates the control actions with the errors of all the outputs as shown in (28)-(30).

$$\mathbf{x}^{*c1} = arg \min_{\mathbf{x}^{c1}} J(\mathbf{x}^{c1}) \tag{28}$$

$$\mathbf{x}^{*c2} = arg \min_{\mathbf{x}^{c2}} J(\mathbf{x}^{c2}) \tag{29}$$

$$J(\mathbf{x}^{c1}) = J(\mathbf{x}^{c2}) = \int_0^{t_f} \left(e_1^2 + e_2^2 + u_1^2 + u_2^2 \right) |_{r_1=1}^{r_2=0} \, dt + \int_0^{t_f} \left(e_1^2 + e_2^2 + u_1^2 + u_2^2 \right) |_{r_1=0}^{r_2=1} \, dt \tag{30}$$

where, $e_1 = r_1 - y_1$ and $e_2 = r_2 - y_2$, are the errors of each output with respect to the established set point, and u_1, u_2 are the control efforts. The PIs controllers obtained by optimizing (28) and (29) for both design concepts are shown in Table 1.

TABLE 1. Mc Avoy DRGA diagonal and off-diagonal PIs controllers with their performances in *J*(x).

DRGA PI off-diagonal		DRGA PI Diagonal	
$K_1{}^{c2}$	-0.363	$K_1{}^{c1}$	0,194
$Ti_1{}^{c2}$	7.9	Ti_1^{c1}	123.6
$K_2{}^{c2}$	0.641	$K_2{}^{c1}$	0.49
$Ti_2{}^{c2}$	628.4	$Ti_2{}^{c1}$	174.4
$J(\mathbf{x}^{c2})$	205.6	$J(\mathbf{x}^{c1})$	224.9

The system responses for the diagonal and off-diagonal PIs controllers are shown in Fig. 5. To establish a coherent comparison framework and analyze the controllers proposed in Table 1, the integral of the squared error (ISE) associated with each output is evaluated, and the integral of the control action (ISU) associated with each input. Results are shown in Table 2.

Table 1 shows that $J(\mathbf{x}^{c2}) < J(\mathbf{x}^{c1})$, which means that from the approach proposed in [11] the off-diagonal pairing is preferable to the diagonal pairing to control the proposed system in (18). When observing Table 2 it can also be noted that the ISE in the output y_2 of the off-diagonal controller shows a marked improvement compared to the diagonal, but in output y_1 the opposite occurs. Something similar occurs when evaluating the ISU for each control effort.

The off-diagonal controller has minimized $J(\mathbf{x}^{c2})$, prioritizing the minimization of the error e_2 and sacrificing e_1, u_1,

TABLE 2. Evaluation of the ISE and ISU for the Mc Avoy DRGA diagonal and off-diagonal controllers of Table 1. The best results are highlighted in bold.

Set Points	$\int(\cdot)^2$	DRGA off-diagonal	DRGA diagonal
	e_1	57.344	**50.501**
$r_1 = 1$	e_2	**0.648**	34.783
$r_2 = 0$	u_1	29.430	**28.077**
	u_2	45.042	**35.766**
	e_1	28.492	**7.825**
$r_1 = 0$	e_2	**6.782**	31.547
$r_2 = 1$	u_1	8.490	**1.431**
	u_2	**29.430**	34.929

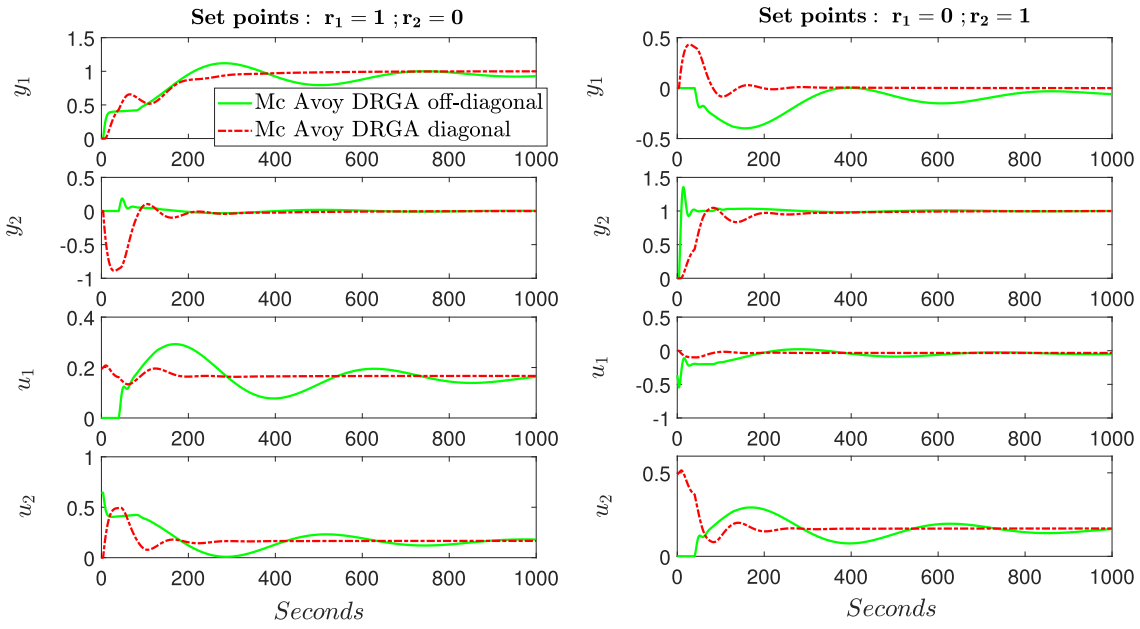

FIGURE 5. System responses for the controllers described in Table 1.

u_2, whose values are greater than for the diagonal controller (see Table 2). These details are not detected if only the value of J is analyzed, because they have been hidden when adding the ISE and ISU in a single design objective. To decide which loop pairing is preferable for a designer, without considering all the a priori preferences, several scenarios are proposed. These scenarios will be analyzed with the proposed multi-objective approach.

A. FIRST SCENARIO

By using the methodology proposed in stage A, two design objectives are stated for the MOP. An objective that agglutinates control efforts and another objective which aggregates the errors of the outputs. Besides, the diagonal design concept ($k = 1$), and off-diagonal design concept ($k = 2$) are considered (see definitions of the concepts in equations (20) and (24)). These design concepts remain fixed for all examples of this paper. The MOP can be proposed as in (31)-(37).

$$\min_{\mathbf{x}^{ck}} \mathbf{J}(\mathbf{x}^{ck}) \tag{31}$$

$$\mathbf{J}(\mathbf{x}^{ck}) = \{J_1(\mathbf{x}^{ck}), J_2(\mathbf{x}^{ck})\} \tag{32}$$

$$J_1(\mathbf{x}^{ck}) = \int_0^{t_f} \left(e_1^2 + e_2^2\right)|_{r_1=1}^{r_2=0}\, dt + \int_0^{t_f} \left(e_1^2 + e_2^2\right)|_{r_1=0}^{r_2=1}\, dt \tag{33}$$

$$J_2(\mathbf{x}^{ck}) = \int_0^{t_f} \left(u_1^2 + u_2^2\right)|_{r_1=1}^{r_2=0}\, dt + \int_0^{t_f} \left(u_1^2 + u_2^2\right)|_{r_1=0}^{r_2=1}\, dt \tag{34}$$

$$t_f = 1000\ seconds$$

$$\underline{\mathbf{x}}^{ck} \leq \mathbf{x}^{ck} \leq \overline{\mathbf{x}}^{ck} \tag{35}$$

TABLE 3. Bounds of the decision vectors $\mathbf{x^{c1}}$ and $\mathbf{x^{c2}}$.

Bounds of $\mathbf{x}^{ck}$				
$\mathbf{x}^{c1}$	K_1^{c1}	Ti_1^{c1}	K_2^{c1}	Ti_2^{c1}
$\underline{\mathbf{x}}^{c1}$	0.01	1	0.01	1
$\overline{\mathbf{x}}^{c1}$	1	1000	1	1000
$\mathbf{x}^{c2}$	K_1^{c2}	Ti_1^{c2}	K_2^{c2}	Ti_2^{c2}
$\underline{\mathbf{x}}^{c2}$	-1	1	0.1	1
$\overline{\mathbf{x}}^{c2}$	-0.1	200	10	1000

TABLE 4. Design objectives for the Mc Avoy DRGA diagonal and off-diagonal controllers for the first scenario.

DRGA PI off-diagonal		DRGA PI diagonal	
$J_1(\mathbf{x}^{c2})$	**93.27**	$J_1(\mathbf{x}^{c1})$	124.7
$J_2(\mathbf{x}^{c2})$	112.3	$J_2(\mathbf{x}^{c1})$	**100.2**
$\sum_{q=1}^{2} J_q(\mathbf{x}^{c2})$	205.6	$\sum_{q=1}^{2} J_q(\mathbf{x}^{c1})$	224.9

$$J_1(\mathbf{x}^{ck}) \leq 300; J_2(\mathbf{x}^{ck}) \leq 150 \tag{36}$$

$$\mathbf{x}^{ck} = \left[K_1^{ck}, Ti_1^{ck}, K_2^{ck}, Ti_2^{ck}\right] \tag{37}$$

The bounds of decision vectors $\mathbf{x}^{c1}$ and $\mathbf{x}^{c2}$ are described in Table 3, and they remain fixed for all scenarios. The optimized design objectives (stage B) of the McAvoy DRGA diagonal and off-diagonal controllers are presented in Table 4. The Pareto fronts for each design concept (stage C) are shown in Fig. 6.

There are three zones in the Pareto fronts, A, B and C (see Fig. 6). Zone A is covered only by the off-diagonal concept. In zone A are the controllers with better performances in their outputs, but with greater control efforts. The off-diagonal controller in *PA* is selected to show this conflict (see objectives J_1 and J_2 in Table 5).

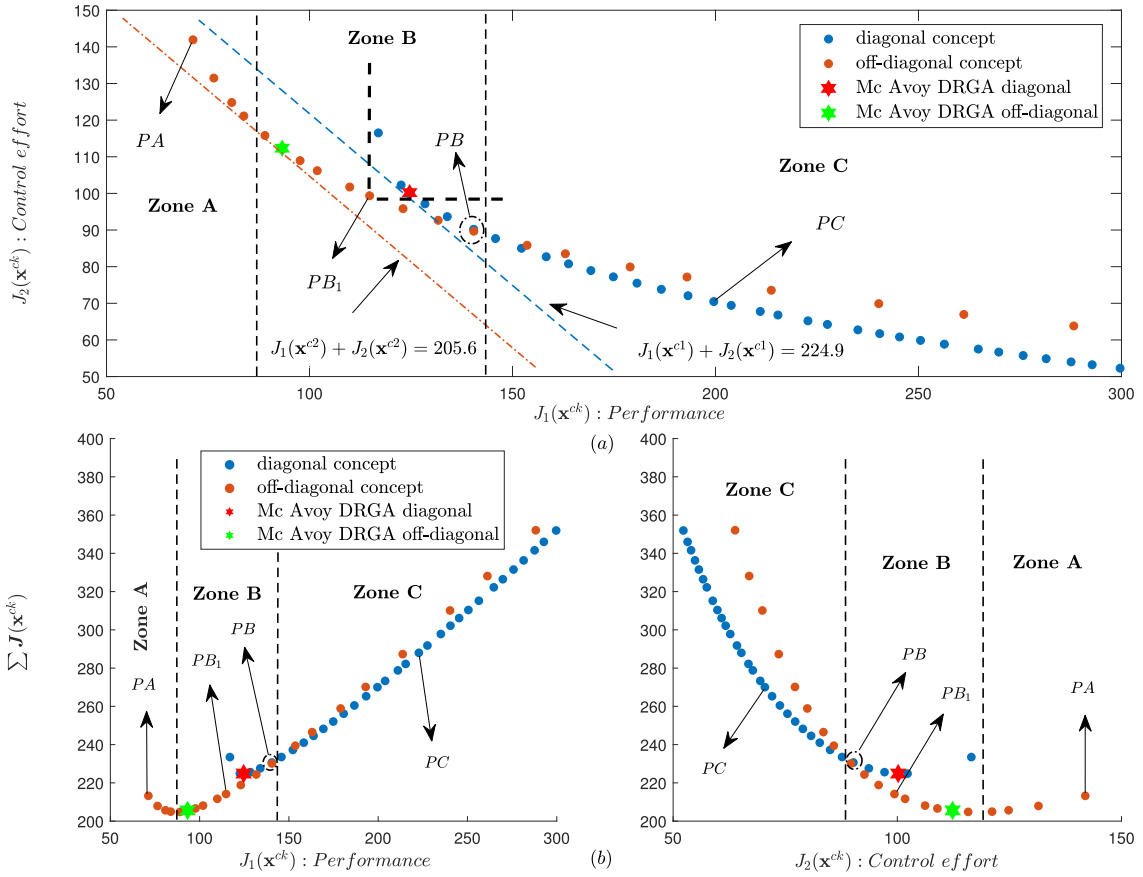

FIGURE 6. Pareto fronts and comparison of design concepts using *level diagrams* for the first scenario. The points PA, PB and PC, have been selected to analyze their trade-offs. The performance of the controllers proposed in [11] are shown in red hexagram (DRGA diagonal) and green hexagram (DRGA off-diagonal). (a) Pareto fronts for diagonal and off-diagonal concepts. (b) Pareto fronts using LD with 1-norm without normalizing.

TABLE 5. PIs diagonal and off-diagonal controllers in PA, PB and PC. The performance of each is shown in *J*(x).

PIs off-diagonal controllers			PIs diagonal controllers		
Parameters	*PA*	*PB*	*Parameters*	*PB*	*PC*
K_1^{c2}	-0.427	-0.353	K_1^{c1}	0.185	0.188
Ti_1^{c2}	7.49	8.213	Ti_1^{c1}	172.4	351.6
K_2^{c2}	0.927	0.4544	K_2^{c1}	0.435	0.38
Ti_2^{c2}	612.8	869.1	Ti_2^{c1}	211.6	394.5
$J_1(\mathbf{x}^{c2})$	71.3	140.5	$J_1(\mathbf{x}^{c1})$	140.4	199.6
$J_2(\mathbf{x}^{c2})$	141.9	89.67	$J_2(\mathbf{x}^{c1})$	90.2	70.47
$\sum_{q=1}^{2} J_q(\mathbf{x}^{c2})$	213.2	230.17	$\sum_{q=1}^{2} J_q(\mathbf{x}^{c1})$	230.6	270.07

In Zone B the off-diagonal concept dominates the diagonal concept. In this zone it is possible to find an off-diagonal controller that dominates the McAvoy DRGA diagonal controller, for example in PB_1. Table 4 shows that the DRGA off-diagonal controller has smaller errors in the outputs than the diagonal controller because $J_1(\mathbf{x}^{c2}) < J_1(\mathbf{x}^{c1})$, but also presents greater control efforts because $J_2(\mathbf{x}^{c2}) > J_2(\mathbf{x}^{c1})$. Considering a multi-objective approach and analyzing the design objectives of the MOP individually, it can be said that the DRGA off-diagonal controller does not dominate the DRGA diagonal controller.

The DRGA diagonal and off-diagonal controllers belong to the Pareto fronts. They are obtained by intersecting with each front the lines $J_1(\mathbf{x}^{ck}) + J_2(\mathbf{x}^{ck}) = L$. The value L is constant, and $L = \sum_{q=1}^{2} J_q(\mathbf{x}^{c1}) = 224.9$ for the DRGA diagonal controller and $L = \sum_{q=1}^{2} J_q(\mathbf{x}^{c1}) = 205.6$ for the DRGA off-diagonal controller (see Fig. 6 (a)).

In Zone C, the diagonal concept dominates the off-diagonal concept. This zone corresponds to the controllers with lesser control efforts but with greater errors in the outputs. An example that shows this conflict is the diagonal controller in *PC* and its objectives are shown in Table 5.

The ISE and ISU of the controllers in PA, PB, PC are shown in Table 6, and their responses in Fig. 7 and Fig. 8. The off-diagonal controller in *PA* compared with the diagonal controller in *PC* presents a better performance in the outputs y_1 and y_2 (see Table 6, in bold). Only the diagonal controller in *PC* is better for controlling the output y_1 when it follows the set point $r_1 = 0, r_2 = 1$. The best performance of the off-diagonal controller in *PA* has a disadvantage given that its control effort has worsened. Its oscillatory behavior can be observed in Fig. 7. The responses of the controllers in *PB* are shown in Fig. 8. It is possible to observe in Table 6 that the diagonal controller in *PB* has a better performance in the output y_1, and the off-diagonal controller in *PB* has a better performance in output y_2.

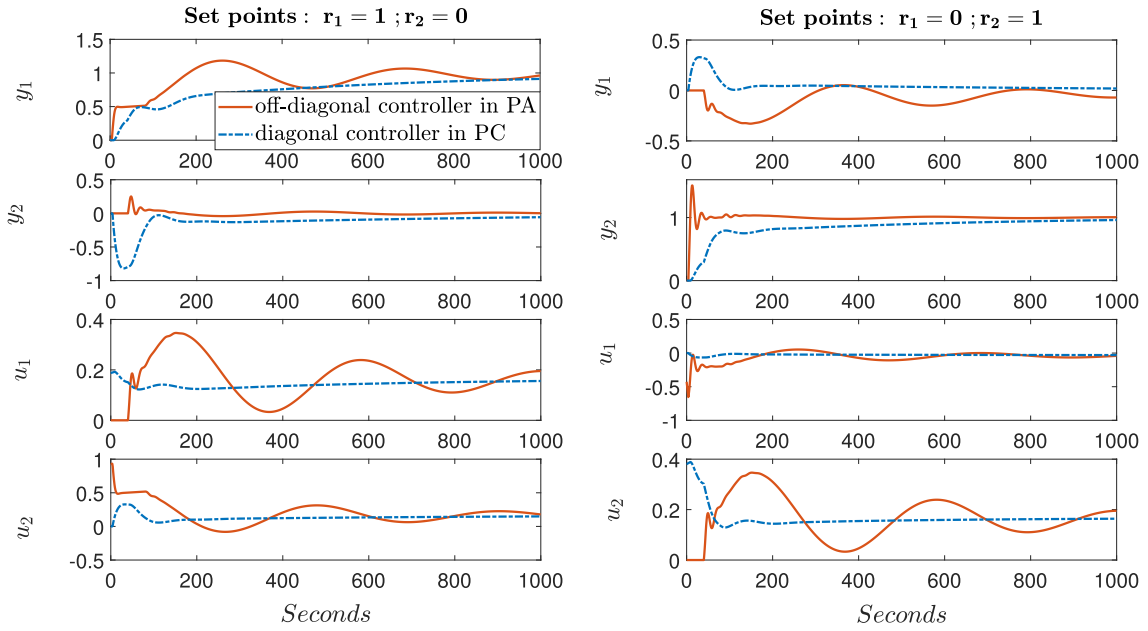

FIGURE 7. Off-diagonal controller response in PA and diagonal in PC corresponding to zones A and C.

TABLE 6. Evaluation of the ISE and ISU for the controllers in PA, PB and PC.

Set Points	$\int(\cdot)^2$	PIs off-diagonal		PIs diagonal	
		PA	PB	PB	PC
$r_1 = 1$ $r_2 = 0$	e_1	**44.920**	82.687	**64.581**	101.652
	e_2	**0.920**	**0.385**	33.065	39.301
	u_1	35.034	**23.721**	25.677	**20.523**
	u_2	62.803	33.073	**30.106**	**20.134**
$r_1 = 0$ $r_2 = 1$	e_1	18.262	51.01	**6.811**	**6.058**
	e_2	**7.609**	**6.804**	36.382	52.971
	u_1	9.291	9.239	**1.204**	**0.805**
	u_2	35.034	**23.721**	33.278	**29.055**

The controllers in PB of both design concepts have a $J_1(\mathbf{x}^{c1}) \approx J_1(\mathbf{x}^{c2})$ and a $J_2(\mathbf{x}^{c1}) \approx J_2(\mathbf{x}^{c2})$. Nevertheless, it can be seen in Fig. 8 that their outputs are very different. These characteristics are not detectable when considering only two objectives and it can be worthwhile to make a final decision and offer a solution for the MOP. For this reason, and knowing that this scenario has the advantage of a simple decision making process for analyzing the MOP, it can be interesting to continue disaggregating the MOP by defining a new scenario in stage A to analyze in detail the trade-off between design objectives (controller responses).

B. SECOND SCENARIO

In this scenario, the MOP with four design objectives is proposed (stage A). The errors of each output are not mixed, and now they constitute two independent objectives, and the other two objectives are the control efforts of each input. The MOP is defined as (38)-(46).

$$\min_{\mathbf{x}^{ck}} \mathbf{J}(\mathbf{x}^{ck}) \tag{38}$$

$$\mathbf{J}(\mathbf{x}^{ck}) = \{J_1(\mathbf{x}^{ck}), J_2(\mathbf{x}^{ck}), J_3(\mathbf{x}^{ck}), J_4(\mathbf{x}^{ck})\} \tag{39}$$

TABLE 7. Design objectives for the Mc Avoy DRGA diagonal and off-diagonal controllers of the second scenario.

DRGA PI off-diagonal		DRGA PI diagonal	
$J_1(\mathbf{x}^{c2})$	85.84	$J_1(\mathbf{x}^{c1})$	**58.33**
$J_2(\mathbf{x}^{c2})$	**7.43**	$J_2(\mathbf{x}^{c1})$	66.33
$J_3(\mathbf{x}^{c2})$	37.87	$J_3(\mathbf{x}^{c1})$	**29.51**
$J_4(\mathbf{x}^{c2})$	74.47	$J_4(\mathbf{x}^{c1})$	**70.70**
$\sum_{q=1}^{4} J_q(\mathbf{x}^{c2})$	205.6	$\sum_{q=1}^{4} J_q(\mathbf{x}^{c1})$	224.9

$$J_1(\mathbf{x}^{ck}) = \int_0^{t_f} e_1^2|_{r_1=1}^{r_2=0}\, dt + \int_0^{t_f} e_1^2|_{r_1=0}^{r_2=1}\, dt \tag{40}$$

$$J_2(\mathbf{x}^{ck}) = \int_0^{t_f} e_2^2|_{r_1=1}^{r_2=0}\, dt + \int_0^{t_f} e_2^2|_{r_1=0}^{r_2=1}\, dt \tag{41}$$

$$J_3(\mathbf{x}^{ck}) = \int_0^{t_f} u_1^2|_{r_1=1}^{r_2=0}\, dt + \int_0^{t_f} u_1^2|_{r_1=0}^{r_2=1}\, dt \tag{42}$$

$$J_4(\mathbf{x}^{ck}) = \int_0^{t_f} u_2^2|_{r_1=1}^{r_2=0}\, dt + \int_0^{t_f} u_2^2|_{r_1=0}^{r_2=1}\, dt \tag{43}$$

$$t_f = 1000\ seconds$$

$$\underline{\mathbf{x}}^{ck} \leq \mathbf{x}^{ck} \leq \overline{\mathbf{x}}^{ck} \tag{44}$$

$$\{J_1(\mathbf{x}^{ck}), J_2(\mathbf{x}^{ck}), J_3(\mathbf{x}^{ck}), J_4(\mathbf{x}^{ck})\} \leq 300 \tag{45}$$

$$\mathbf{x}^{ck} = \left[K_1^{ck}, Ti_1^{ck}, K_2^{ck}, Ti_2^{ck}\right] \tag{46}$$

The performance of the McAvoy DRGA diagonal and off-diagonal controllers are shown in Table 7 (stage B). The DRGA diagonal controller is better in three of the four design objectives (J_1, J_3, J_4), compared to the DRGA off-diagonal controller (see Table 7).

The Pareto fronts of the diagonal design concept ($\mathbf{x}^{c1}$) and the off-diagonal design concept ($\mathbf{x}^{c2}$) are shown in Fig. 9 (a) and (b) respectively. The comparison of both design concepts when applying the QI quality indicator is

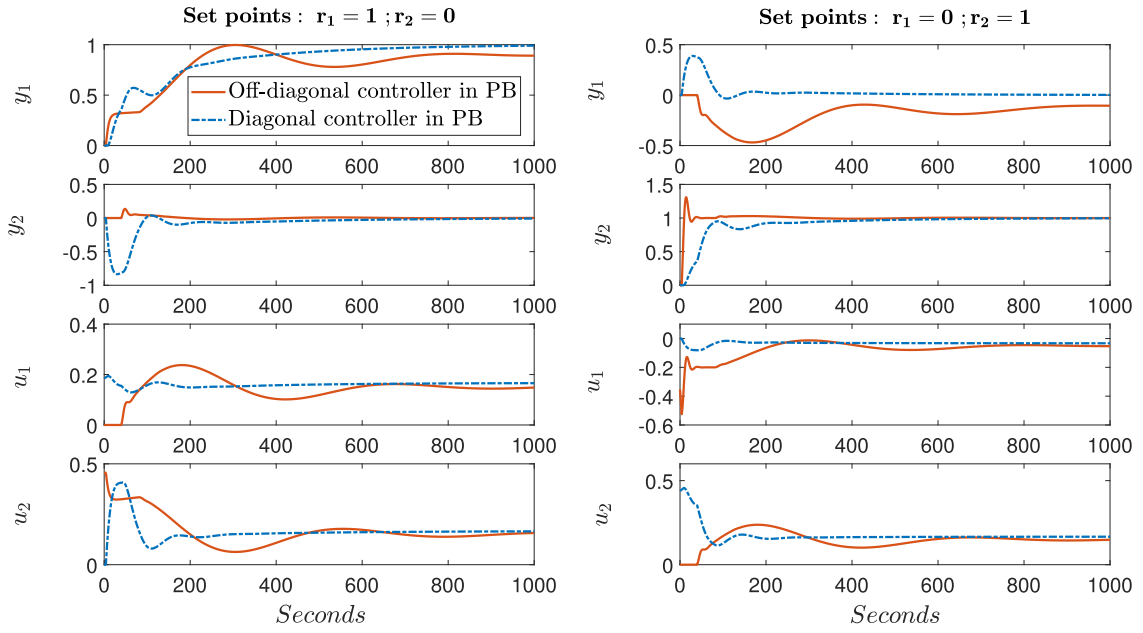

FIGURE 8. Diagonal and off-diagonal controllers responses in PB corresponding to zone B.

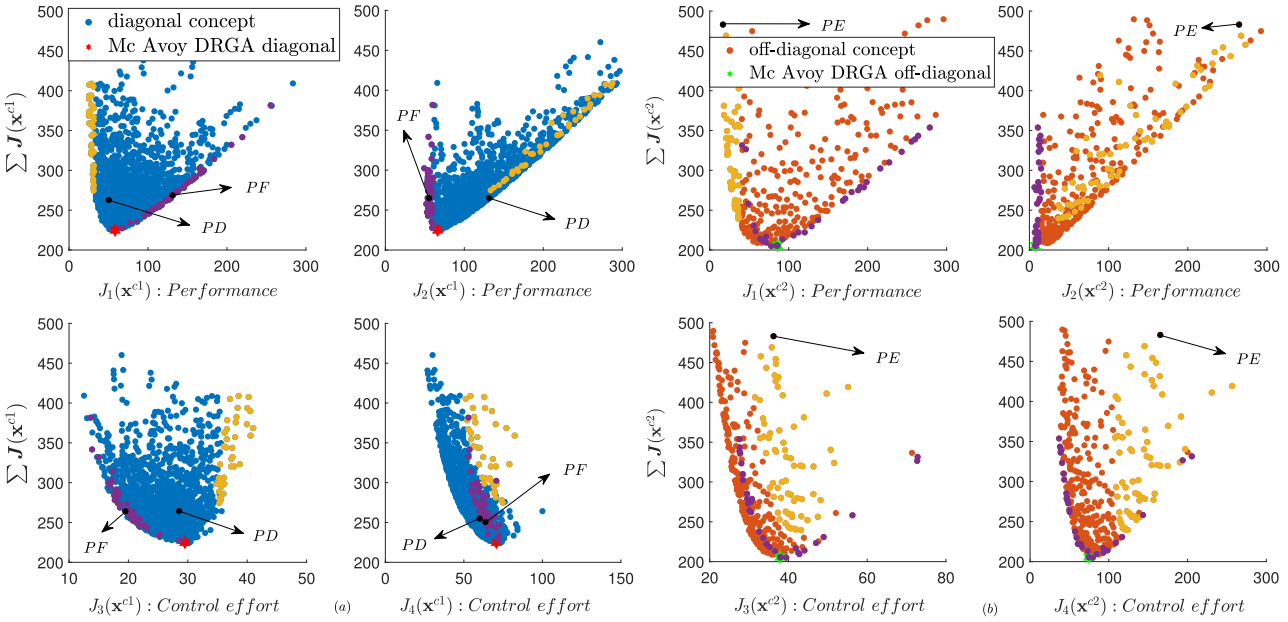

FIGURE 9. Pareto fronts of the diagonal and off-diagonal design concepts using 1-norm without normalizing. (a) Diagonal concept. (b) Off-diagonal concept.

shown in Fig. 10 (a). The Pareto fronts with 1-norm without normalizing $\sum_{i=1}^{4} J_i(\mathbf{x}^{ck})$ in both design concepts are shown in Fig. 10 (b) (stage C).

With the proposed multi-objective approach, the diagonal controller in *PD* is better in J_1, J_3, and J_4 than the McAvoy DRGA controller off-diagonal (this controller minimizes the error in the output y_2, i.e. J_2) (see Table 7 and Table 8). The controller in *PD* is also better in J_2, J_3, J_4, than the controller in *PE* (this controller minimizes the error in the output y_1, i.e. J_1). The controller in *PF* has prioritized minimizing the control efforts of each input (i.e. J_3, J_4) (see Table 8). The responses of these controllers are shown in Fig. 11.

In Fig. 9 (a), the yellow solutions in the design objectives J_1 and J_2 reveals that the diagonal design concept has a conflict between these objectives.

The conflict between J_1 and J_2 implies that improving the performance at output y_1 has the consequence of worsening the performance at output y_2. The opposite is also true, and it is shown in the purple solutions in the same objectives. There is also conflict between objectives J_1 and J_3 and between

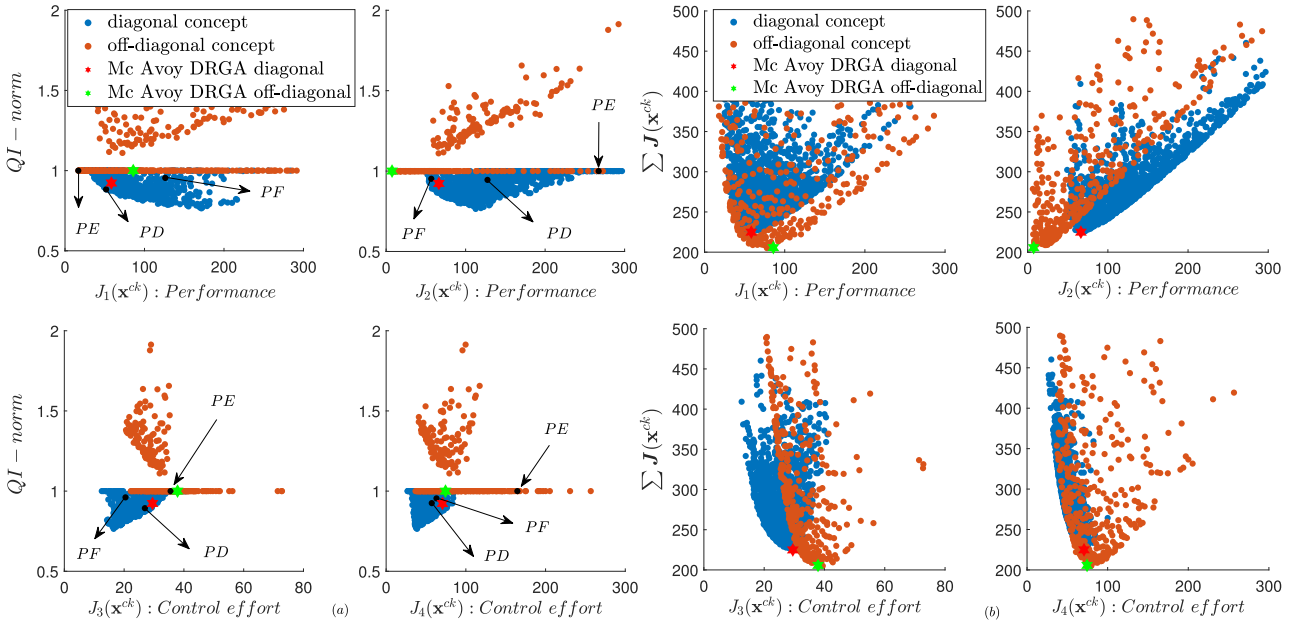

FIGURE 10. Comparison of design concepts using *level diagrams* for scenario 2. The solutions PD, PE, PF, were selected to analyze their response. (a) Design concepts using LD with QI-norm. (b) Design concepts using LD with 1-norm without normalizing.

TABLE 8. PIs controllers in PD, PE, PF, shown in Fig. 9 and Fig. 10. Their performances are compared according to the objectives $J(\mathbf{x})$, and the best results are highlighted in bold.

PI off-diagonal controller		PIs diagonal controllers		
Parameters	*PE*	*Parameters*	*PD*	*PF*
K_1^{c2}	0.612	K_1^{c1}	0.335	0.171
Ti_1^{c2}	122.52	Ti_1^{c1}	324.31	370.83
K_2^{c2}	0.432	K_2^{c1}	0.391	0.597
Ti_2^{c2}	613.45	Ti_2^{c1}	439.70	277.18
$J_1(\mathbf{x}^{c2})$	**16.74**	$J_1(\mathbf{x}^{c1})$	52.97	126.11
$J_2(\mathbf{x}^{c2})$	264.77	$J_2(\mathbf{x}^{c1})$	**126.35**	**55.25**
$J_3(\mathbf{x}^{c2})$	36.20	$J_3(\mathbf{x}^{c1})$	**28.54**	**19.50**
$J_4(\mathbf{x}^{c2})$	165.33	$J_4(\mathbf{x}^{c1})$	**56.53**	**63.16**
$\sum_{q=1}^{4} J_q(\mathbf{x}^{c2})$	483.04	$\sum_{q=1}^{4} J_q(\mathbf{x}^{c1})$	264.39	264.03

J_2 and J_4, that is, between each of their input-output pairings (see controllers in *PD* and in *PF* in Table 8).

The tuning parameters and the performance of the diagonal controllers in *PD*, *PF*, (with different trade-off between objectives) and the off-diagonal controller in *PE* (with the best performance in J_1) are shown in Table 8 and in Fig. 9 and Fig. 10.

The yellow solutions in Fig. 9 (b) indicate that in the off-diagonal design concept there is also conflict between the performances of outputs y_1 and y_2 (J_1 and J_2). The relationship that exists between the performances of each output and its control efforts are shown in the purple solutions in the objectives (J_1 and J_3), (J_2 and J_4). The best performances at output y_2 correspond to the greatest control efforts (see J_2 and J_4 of controller DRGA off-diagonal in Table 7). The same occurs between the best performance of the output y_1 and its control effort u_1 (see J_1 and J_3 of the controller in *PE* in Table 8). These conflicts are also evident in the responses of the controllers shown in Fig. 11.

An interesting aspect that shows this scenario with greater clarity is that when comparing the design concepts it is observed that there is a wide region where the diagonal concept is preferable to off-diagonal. The region where the diagonal design concept is preferable to the off-diagonal concept corresponds to values where $QI < 1$ (see (a) in Fig. 10).

The ISE and the ISU were evaluated for the controllers in *PD*, *PE*, and *PF* (see Table 9). Although in this scenario it is possible to observe the errors in each of the outputs and their control efforts for each set point r_1 and r_2, it is not feasible to know the relation of conflictivity of each independently. This scenario has a more complex decision making process, but it has the advantage that it provides more information about the compensation that occurs between the MOP design objectives than the first scenario. This scenario shows that the off-diagonal concept is preferable over the diagonal concept only when there is a very strong preference to minimize J_2.

To analyze the conflicts and performance of the outputs and control actions for each set point independently, it is feasible to go back to stage A of the methodology and generate a scenario with eight design objectives such as the one proposed in third scenario.

C. THIRD SCENARIO

In this scenario, the MOP with eight design objectives is proposed. The errors associated with each of the outputs are analyzed completely independently as well as the control efforts of each of the inputs. A step in each set points r_1 and r_2 is applied. Therefore, the MOP is defined as (47)-(55).

$$\min_{\mathbf{x}^{ck}} \mathbf{J}(\mathbf{x}^{ck}) \tag{47}$$

$$\mathbf{J}(\mathbf{x}^{ck}) = \{J_1(\mathbf{x}^{ck}), J_2(\mathbf{x}^{ck}), J_3(\mathbf{x}^{ck}), J_4(\mathbf{x}^{ck}), J_5(\mathbf{x}^{ck}), J_6(\mathbf{x}^{ck}), J_7(\mathbf{x}^{ck}), J_8(\mathbf{x}^{ck})\} \tag{48}$$

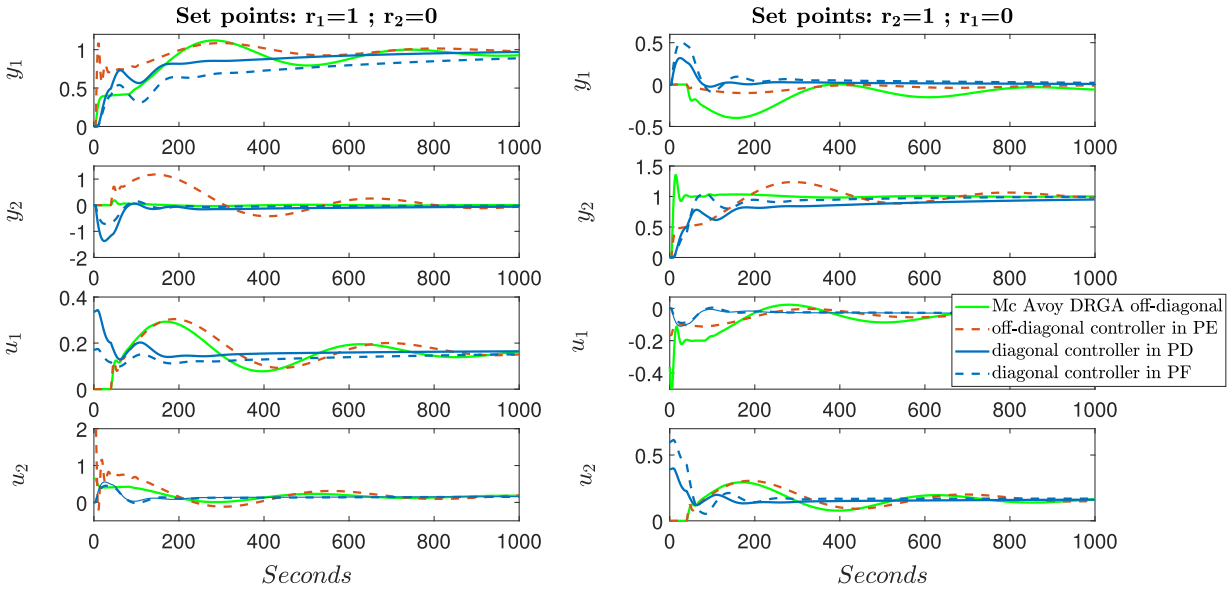

FIGURE 11. Responses of the selected controllers in PD, PE, PF, compared with the DRGA off-diagonal controller proposed in [11].

TABLE 9. Evaluation of the ISE and ISU for the controllers selected in PD, PE, PF. The comparison between them is shown in bold.

Set Points	$\int(\cdot)^2$	PI off-diagonal	PIs diagonal	
		PE	PD	PF
	e_1	**14.83**	49.35	114.37
$r_1 = 1$	e_2	223.56	**77.79**	**21.97**
$r_2 = 0$	u_1	33.22	**27.39**	**18.53**
	u_2	133.61	**29.42**	**24.59**
	e_1	**2.12**	3.82	11.94
$r_1 = 0$	e_2	41.42	48.76	**33.48**
$r_2 = 1$	u_1	2.99	**1.18**	**0.984**
	u_2	33.22	**27.15**	38.66

$$J_1(\mathbf{x}^{ck}) = \int_0^{t_f} e_1^2|_{r_1=1}^{r_2=0}\, dt;\ J_2(\mathbf{x}^{ck}) = \int_0^{t_f} e_2^2|_{r_1=1}^{r_2=0}\, dt \tag{49}$$

$$J_3(\mathbf{x}^{ck}) = \int_0^{t_f} e_1^2|_{r_1=0}^{r_2=1}\, dt;\ J_4(\mathbf{x}^{ck}) = \int_0^{t_f} e_2^2|_{r_1=0}^{r_2=1}\, dt \tag{50}$$

$$J_5(\mathbf{x}^{ck}) = \int_0^{t_f} u_1^2|_{r_1=1}^{r_2=0}\, dt;\ J_6(\mathbf{x}^{ck}) = \int_0^{t_f} u_2^2|_{r_1=1}^{r_2=0}\, dt \tag{51}$$

$$J_7(\mathbf{x}^{ck}) = \int_0^{t_f} u_1^2|_{r_1=0}^{r_2=1}\, dt;\ J_8(\mathbf{x}^{ck}) = \int_0^{t_f} u_2^2|_{r_1=0}^{r_2=1}\, dt \tag{52}$$

$$t_f = 1000\ seconds$$

$$\underline{\mathbf{x}}^{ck} \leq \mathbf{x}^{ck} \leq \overline{\mathbf{x}}^{ck} \tag{53}$$

$$\{J_1(\mathbf{x}^{ck}), J_2(\mathbf{x}^{ck}), J_3(\mathbf{x}^{ck}), J_4(\mathbf{x}^{ck}), J_5(\mathbf{x}^{ck}), \times J_6(\mathbf{x}^{ck}), J_7(\mathbf{x}^{ck}), J_8(\mathbf{x}^{ck})\} \leq 300 \tag{54}$$

$$\mathbf{x}^{ck} = \left[K_1^{ck}, Ti_1^{ck}, K_2^{ck}, Ti_2^{ck}\right] \tag{55}$$

The performances of the McAvoy diagonal and off-diagonal controllers are shown in Table 10. The Pareto fronts of this MOP for the diagonal and off-diagonal concepts are shown in Fig. 12 and Fig. 13 respectively.

The yellow and purple stripes in each design concept indicate the conflicts between the design objectives of the MOP (see Figs. 12,13). For the off-diagonal design concept, a conflict between $J_5(\mathbf{x}^{c2})$ and $J_7(\mathbf{x}^{c2})$ is observed (improving one means worsening the other). The conflict between these objectives enables observing that the control effort u_1 is greater when the step signal is applied in r_1 and lower when it is applied in r_2. The objectives $J_6(\mathbf{x}^{c1})$ and $J_8(\mathbf{x}^{c1})$ represent the control effort u_2 of the diagonal design concept, a lower level of conflictivity can be observed than in the off-diagonal concept.

It is important to emphasize that this information was hidden in the first and second scenarios. If a designer or control engineer wants to establish these types of details in the performance of the system he or she should analyze this scenario. For both design concepts, objectives $J_1(\mathbf{x}^{ck})$ and $J_3(\mathbf{x}^{ck})$ represent errors in the output y_1 and $J_2(\mathbf{x}^{ck})$, while $J_4(\mathbf{x}^{ck})$ in the output y_2 does not present any conflict between them. These objectives can be merged to reduce the complexity of the MOP without losing relevant information for the decision-making stage.

Moreover, in Fig. 11 it is important to analyze whether the control efforts of each selected controller are oscillating. To ensure that the optimal controllers improve this aspect it is possible to go back again to stage A and propose a new scenario with new design objectives. In this scenario it will show how modifying design objectives can drastically change the designer's preferences for selecting a certain input-output pairing.

D. FOURTH SCENARIO

The MOP with four design objectives is proposed. The integral of the absolute value of the error (IAE) is used as a performance index for each output, and the integral of the absolute

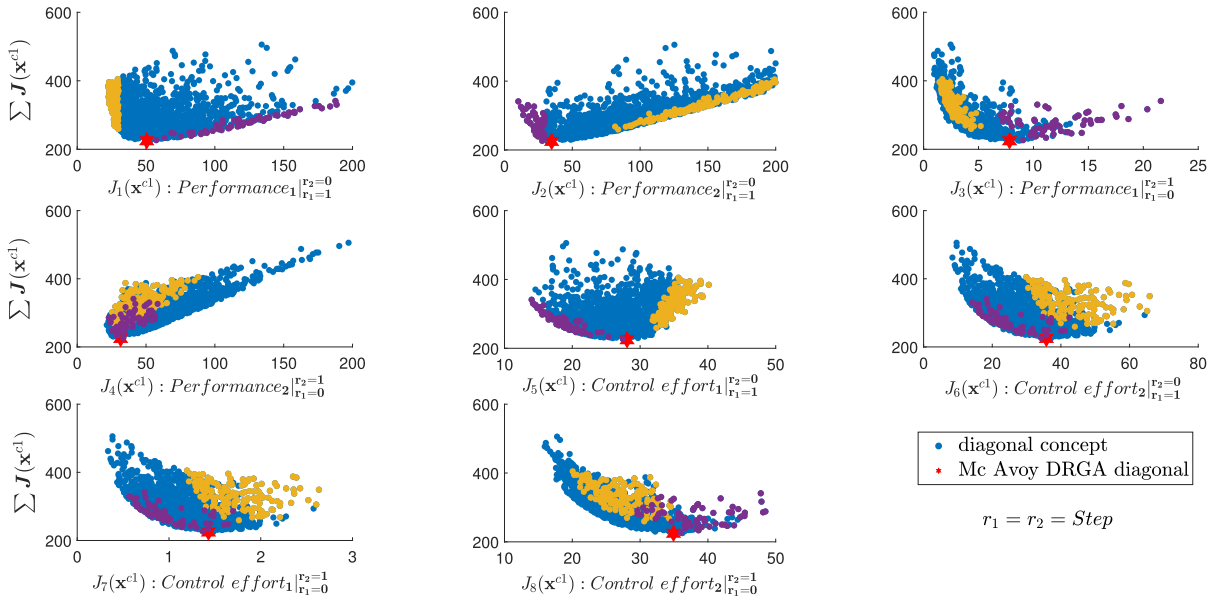

FIGURE 12. Pareto front using 1-norm without normalizing for the diagonal design concept.

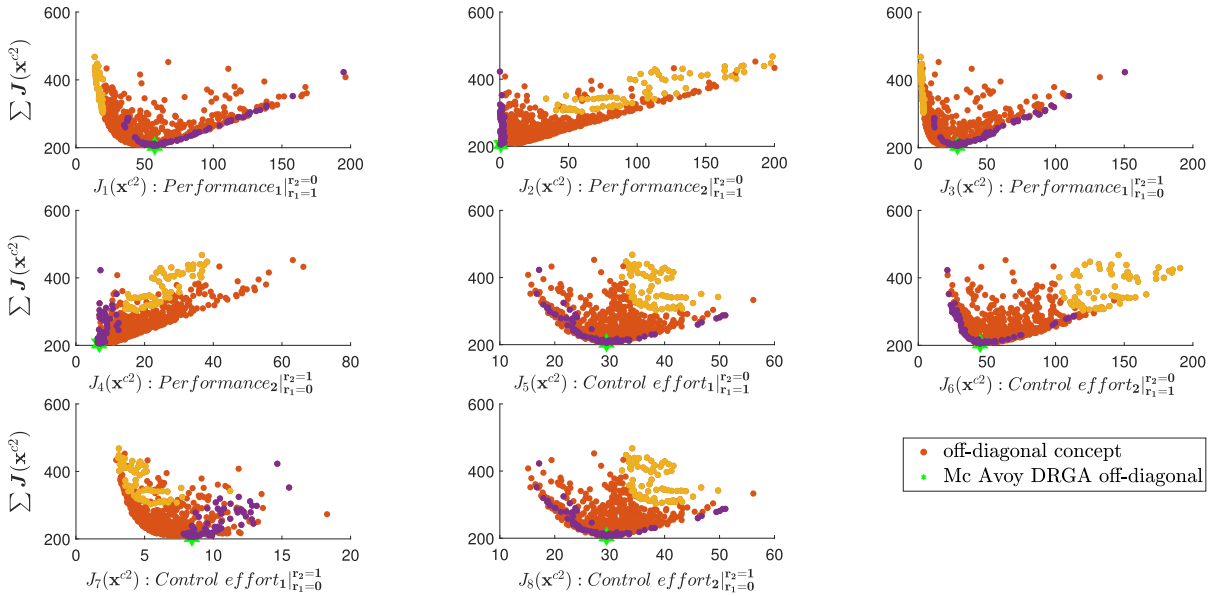

FIGURE 13. Pareto front using 1-norm without normalizing for the off-diagonal design concept.

value of the derivative control signal (IADU) for the control actions. Applying the IAE is intended to give a greater physical sense to analyzing the error for reference input tracking, and avoiding less intuitive squared signals. To decrease the oscillations in the control actions, and as a consequence in the system response, the IADU is proposed. The MOP is proposed as (56)-(64).

$$\min_{\mathbf{x}^{ck}} \mathbf{J}(\mathbf{x}^{ck}) \tag{56}$$

$$\mathbf{J}(\mathbf{x}^{ck}) = \{J_1(\mathbf{x}^{ck}), J_2(\mathbf{x}^{ck}), J_3(\mathbf{x}^{ck}), J_4(\mathbf{x}^{ck})\} \tag{57}$$

$$J_k(\mathbf{x}^{ck}) = \int_0^{t_f} |e_1| \Big|_{r_1=1}^{r_2=0} dt + \int_0^{t_f} |e_1| \Big|_{r_1=0}^{r_2=1} dt \tag{58}$$

$$J_2(\mathbf{x}^{ck}) = \int_0^{t_f} |e_2| \Big|_{r_1=1}^{r_2=0} dt + \int_0^{t_f} |e_2| \Big|_{r_1=0}^{r_2=1} dt \tag{59}$$

$$J_3(\mathbf{x}^{ck}) = \int_0^{t_f} \left|\frac{du_1}{dt}\right| \Big|_{r_1=1}^{r_2=0} dt + \int_0^{t_f} \left|\frac{du_1}{dt}\right| \Big|_{r_1=0}^{r_2=1} dt \tag{60}$$

$$J_4(\mathbf{x}^{ck}) = \int_0^{t_f} \left|\frac{du_2}{dt}\right| \Big|_{r_1=1}^{r_2=0} dt + \int_0^{t_f} \left|\frac{du_2}{dt}\right| \Big|_{r_1=0}^{r_2=1} dt \tag{61}$$

$$t_f = 1000\ seconds$$

$$\underline{\mathbf{x}}^{ck} \leq \mathbf{x}^{ck} \leq \overline{\mathbf{x}}^{ck} \tag{62}$$

$$\{J_1(\mathbf{x}^{ck}), J_2(\mathbf{x}^{ck})\} < 500; \{J_3(\mathbf{x}^{ck}), J_4(\mathbf{x}^{ck})\} < 2 \tag{63}$$

$$\mathbf{x}^{ck} = \left[K_1^{ck}, Ti_1^{ck}, K_2^{ck}, Ti_2^{ck}\right] \tag{64}$$

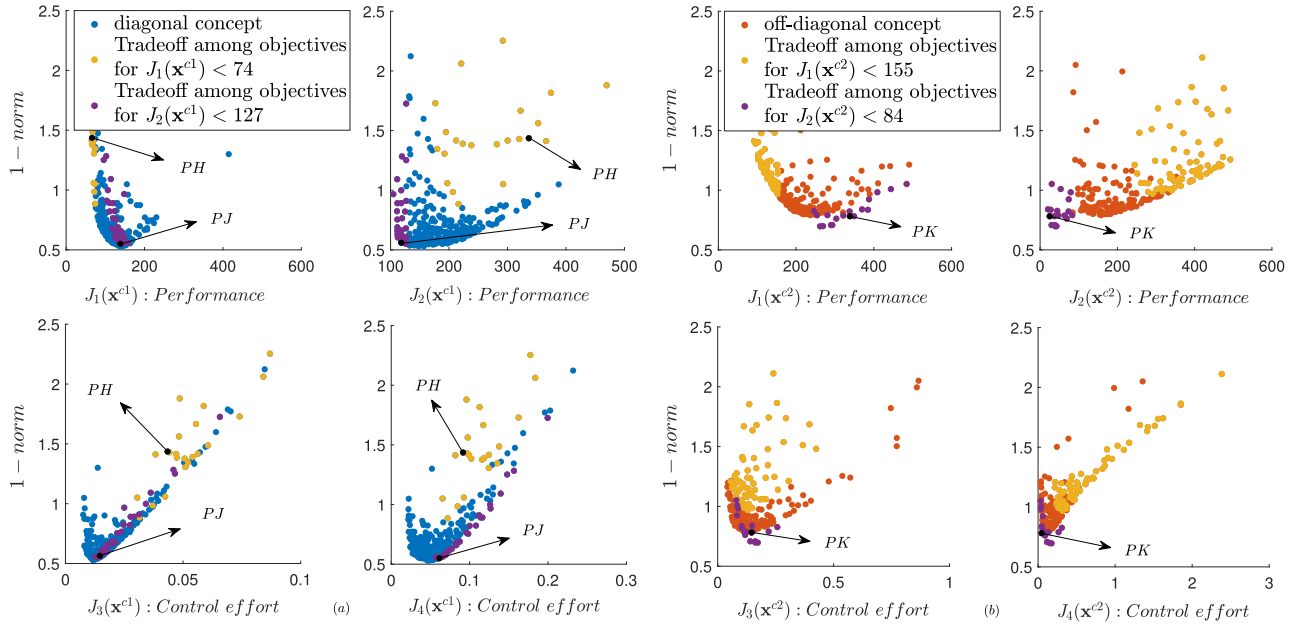

FIGURE 14. Pareto front using 1-norm for the diagonal an off-diagonal design concepts. (a) Diagonal concept. (b) Off-diagonal concept.

TABLE 10. Design objectives for the Mc Avoy DRGA diagonal and off diagonal controllers of the third scenario.

DRGA PI off-diagonal		DRGA PI Diagonal	
$J_1(\mathbf{x}^{c2})$	57.34	$J_1(\mathbf{x}^{c1})$	**50.5**
$J_2(\mathbf{x}^{c2})$	**0.648**	$J_2(\mathbf{x}^{c1})$	34.78
$J_3(\mathbf{x}^{c2})$	28.49	$J_3(\mathbf{x}^{c1})$	**7.83**
$J_4(\mathbf{x}^{c2})$	**6.78**	$J_4(\mathbf{x}^{c1})$	31.55
$J_5(\mathbf{x}^{c2})$	29.43	$J_5(\mathbf{x}^{c1})$	**28.08**
$J_6(\mathbf{x}^{c2})$	45.04	$J_6(\mathbf{x}^{c1})$	**35.77**
$J_7(\mathbf{x}^{c2})$	8.44	$J_7(\mathbf{x}^{c1})$	**1.43**
$J_8(\mathbf{x}^{c2})$	**29.43**	$J_8(\mathbf{x}^{c1})$	34.93
$\sum_{q=1}^{8} J_q(\mathbf{x}^{c2})$	205.6	$\sum_{q=1}^{8} J_q(\mathbf{x}^{c1})$	224.9

The optimized objectives for the controllers in *PH*, *PJ*, and *PK* is shown in Table 11. The Pareto fronts of both design concepts are shown in Fig. 14. The stripes in yellow and purple indicate the trade-offs between the design objectives.

For the diagonal concept, the indicator *QI* presents values below the unit ($QI < 1$), and the off-diagonal concept is above the unit ($QI > 1$). This shows that from the proposed MO approach the diagonal concept is widely preferable to the off-diagonal concept (see Fig. 15 (a)).

The off-diagonal concept would only be preferable in the region where $J_2(\mathbf{x}^{ck}) < 104.8$ is covered only by the off-diagonal design concept. The IAE and IADU values for the controllers in *PH*, *PJ*, *PK* (selected in Fig. 14 and Fig. 15) are shown in Table 12.

As a compromise solution for the MOP, the diagonal controller in *PJ* has been selected because it performs better in three design objectives compared with *PH* and *PK* (see Table 11). The responses of these controllers now have lower oscillations compared to the second and third scenarios (see Fig. 16).

TABLE 11. Controllers selected in PH, PJ, PK of Fig. 14 and Fig. 15. The design objectives (performance) of each controller are compared and highlighted in bold.

Off-diagonal PI		Diagonal PIs		
Parameters	*PK*	*Parameters*	*PH*	*PJ*
K_1^{c2}	-0.3948	K_1^{c1}	0.3527	0.1417
Ti_1^{c2}	9.3481	Ti_1^{c1}	102.04	98.89
K_2^{c2}	0.3649	K_2^{c1}	0.2003	0.2849
Ti_2^{c2}	419.98	Ti_2^{c1}	209.13	99.17
$J_1(\mathbf{x}^{c2})$	338.37	$J_1(\mathbf{x}^{c1})$	**66.06**	140.57
$J_2(\mathbf{x}^{c2})$	**24.80**	$J_2(\mathbf{x}^{c1})$	336.46	118.53
$J_3(\mathbf{x}^{c2})$	0.1460	$J_3(\mathbf{x}^{c1})$	0.0434	**0.0146**
$J_4(\mathbf{x}^{c2})$	0.0809	$J_4(\mathbf{x}^{c1})$	0.0916	**0.0662**
$\sum_{q=1}^{4} J_q(\mathbf{x}^{c2})$	363.40	$\sum_{q=1}^{4} J_q(\mathbf{x}^{c1})$	402.66	**259.18**

TABLE 12. Evaluation of the IAE and IADU for the controllers selected in PH, PJ and PK of Fig. 16. In bold, the IAE and IADU of the controllers are compared.

Set Points	$\int \lvert \cdot \rvert dt$	Off-diagonal PI	Diagonal PIs	
		PK	*PH*	*PJ*
$r_1 = 1$ $r_2 = 0$	e_1	174.03	**53.20**	116.55
	e_2	**9.05**	168.99	60.30
	u_1	0.1927	0.1415	**0.0284**
	u_2	**0.2116**	0.3785	0.2232
$r_1 = 0$ $r_2 = 1$	e_1	164.55	**13.06**	24.22
	e_2	**15.96**	167.67	58.42
	u_1	0.5370	0.0757	**0.0446**
	u_2	0.1927	**0.0795**	0.1077

V. EXAMPLE 2

The 3×3 system proposed in [15], whose model is shown in (65), is used in this section. To control this system, RGA suggests the loop pairing: $y_1 - u_3/y_2 - u_2/y_3 - u_1$ (LP_1); and RNGA a different one: $y_1 - u_2/y_2 - u_3/y_3 - u_1$ (LP_2), see (66) and (67), respectively.

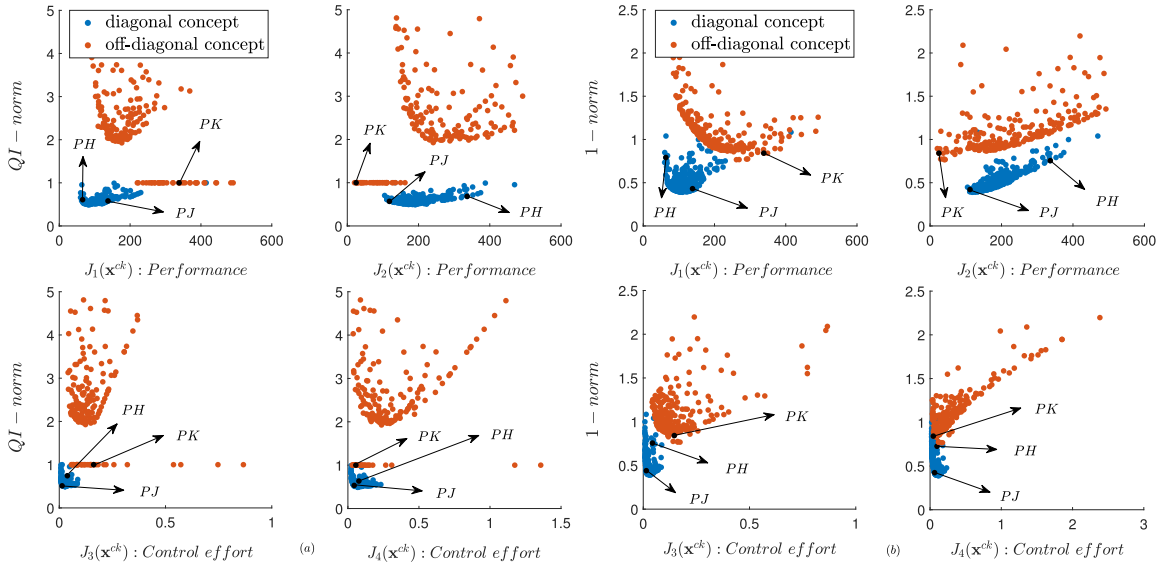

FIGURE 15. Comparison of diagonal and off-diagonal design concepts with the QI indicator and 1-norm. Only solutions where QI < 5 were selected. (a) LD with the QI-norm. (b) LD with the 1-norm.

In order to test both loop pairing alternatives, in [15] decentralized 1-DOF PID controllers are designed based on IMC-PID tuning rule. Simulation results demonstrate that LP_2 is significantly better than LP_1.

In order to carry out a more in-depth study of the problem, the proposed MO methodology is applied, establishing two design concepts, $\mathbf{c}_1$ (loop pairing LP_1) and $\mathbf{c}_2$ (loop pairing LP_2), defined in (68)-(79). In the same way that [15], each loop pairing has associated the design of PID controllers of 1-DOF with derivative filter (N = 100).

$$\begin{bmatrix} y_1(s) \\ y_2(s) \\ y_3(s) \end{bmatrix} = \begin{bmatrix} \dfrac{e^{-9s}}{6s^2+17s+1} & \dfrac{-9e^{-5s}}{s^2+4s+1} & \dfrac{13e^{-3s}}{3s^2+35s+1} \\ \dfrac{-5e^{-13s}}{2s^2+19s+1} & \dfrac{8e^{-2s}}{s^2+33s+1} & \dfrac{7e^{-5s}}{s^2+3s+1} \\ \dfrac{-16e^{-3s}}{s^2+5s+1} & \dfrac{3e^{-7s}}{s^2+14s+1} & \dfrac{e^{-11s}}{3s^2+25s+1} \end{bmatrix} \times \begin{bmatrix} u_1(s) \\ u_2(s) \\ u_3(s) \end{bmatrix} \tag{65}$$

$$\Lambda = \begin{bmatrix} -0.0054 & 0.3981 & \mathbf{0.6073} \\ -0.0992 & \mathbf{0.6912} & 0.4080 \\ \mathbf{1.1046} & -0.0893 & -0.0153 \end{bmatrix} \tag{66}$$

$$\Lambda_\Phi = \begin{bmatrix} -0.0024 & \mathbf{0.9237} & 0.0787 \\ -0.0063 & 0.0829 & \mathbf{0.9235} \\ \mathbf{1.0088} & -0.0066 & -0.0022 \end{bmatrix} \tag{67}$$

$$\mathbf{c}_1 = \left[C^{c_1}_{y_1,\hat{u}_1}, C^{c_1}_{y_2,\hat{u}_2}, C^{c_1}_{y_3,\hat{u}_3} \right] \tag{68}$$

$$L_p^{c_1} = \begin{bmatrix} 0 & 0 & 1 \\ 0 & 1 & 0 \\ 1 & 0 & 0 \end{bmatrix} \tag{69}$$

$$C^{c_1}_{y_1,\hat{u}_1} = K_1^{c1}\left(1 + \frac{1}{Ti_1^{c1}s} + Td_1^{c1}\frac{N}{1+N/s}\right) \tag{70}$$

$$C^{c_1}_{y_2,\hat{u}_2} = K_2^{c1}\left(1 + \frac{1}{Ti_2^{c1}s} + Td_2^{c1}\frac{N}{1+N/s}\right) \tag{71}$$

$$C^{c_1}_{y_3,\hat{u}_3} = K_3^{c1}\left(1 + \frac{1}{Ti_3^{c1}s} + Td_3^{c1}\frac{N}{1+N/s}\right) \tag{72}$$

$$\mathbf{x}^{c1} = \left[K_1^{c1}, Ti_1^{c1}, Td_1^{c1}, K_2^{c1}, Ti_2^{c1}, Td_2^{c1}, K_3^{c1}, Ti_3^{c1}, Td_3^{c1} \right] \tag{73}$$

$$\mathbf{c}_2 = \left[C^{c_2}_{y_1,\hat{u}_1}, C^{c_2}_{y_2,\hat{u}_2}, C^{c_2}_{y_3,\hat{u}_3} \right] \tag{74}$$

$$L_p^{c_2} = \begin{bmatrix} 0 & 0 & 1 \\ 1 & 0 & 0 \\ 0 & 1 & 0 \end{bmatrix} \tag{75}$$

$$C^{c_2}_{y_1,\hat{u}_1} = K_1^{c2}\left(1 + \frac{1}{Ti_1^{c2}s} + Td_1^{c2}\frac{N}{1+N/s}\right) \tag{76}$$

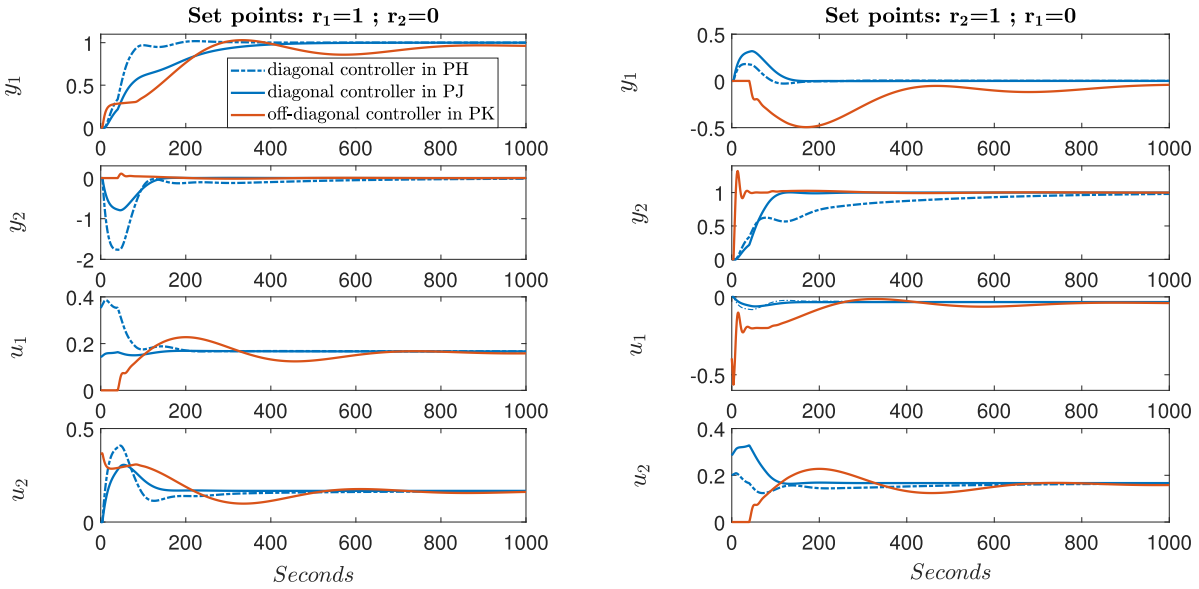

FIGURE 16. Responses of the selected controllers in the Pareto fronts of the fourth scenario.

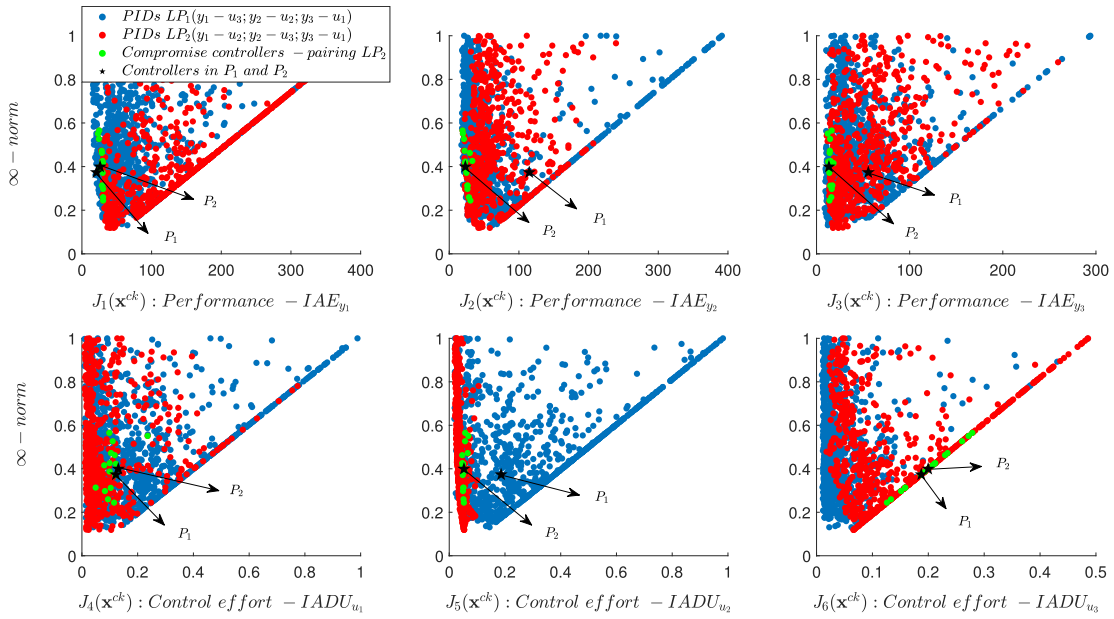

FIGURE 17. Pareto fronts for the loop pairings LP1 and LP2 of the second example.

$$C^{c2}_{y_2,\hat{u}_2} = K_2^{c2}\left(1+\frac{1}{Ti_2^{c2}s}+Td_2^{c2}\frac{N}{1+N/s}\right) \tag{77}$$

$$C^{c2}_{y_3,\hat{u}_3} = K_3^{c2}\left(1+\frac{1}{Ti_3^{c2}s}+Td_3^{c2}\frac{N}{1+N/s}\right) \tag{78}$$

$$\mathbf{x}^{c2} = \left[K_1^{c2}, Ti_1^{c2}, Td_1^{c2}, K_2^{c2}, Ti_2^{c2}, Td_2^{c2}, K_3^{c2}, Ti_3^{c2}, Td_3^{c2}\right] \tag{79}$$

By following the proposed MO methodology, two MOPs are proposed (corresponding to stage A of Fig. 4), $k = 1$ corresponds to loop pairing LP_1 and $k = 2$ to LP_2, see equations (80)-(86). Six design objectives are set for each MOP, allowing an independent evaluation of the performance of the outputs and control efforts (stage B). Here e_η represents the error of each output and u_η the control effort of each input.

$$\min_{\mathbf{x}^{ck}} \mathbf{J}(\mathbf{x}^{ck}) \tag{80}$$

$$\mathbf{J}(\mathbf{x}^{ck}) = \{J_1(\mathbf{x}^{ck}), J_2(\mathbf{x}^{ck}), J_3(\mathbf{x}^{ck}), J_4(\mathbf{x}^{ck}), J_5(\mathbf{x}^{ck}), \times J_6(\mathbf{x}^{ck})\} \tag{81}$$

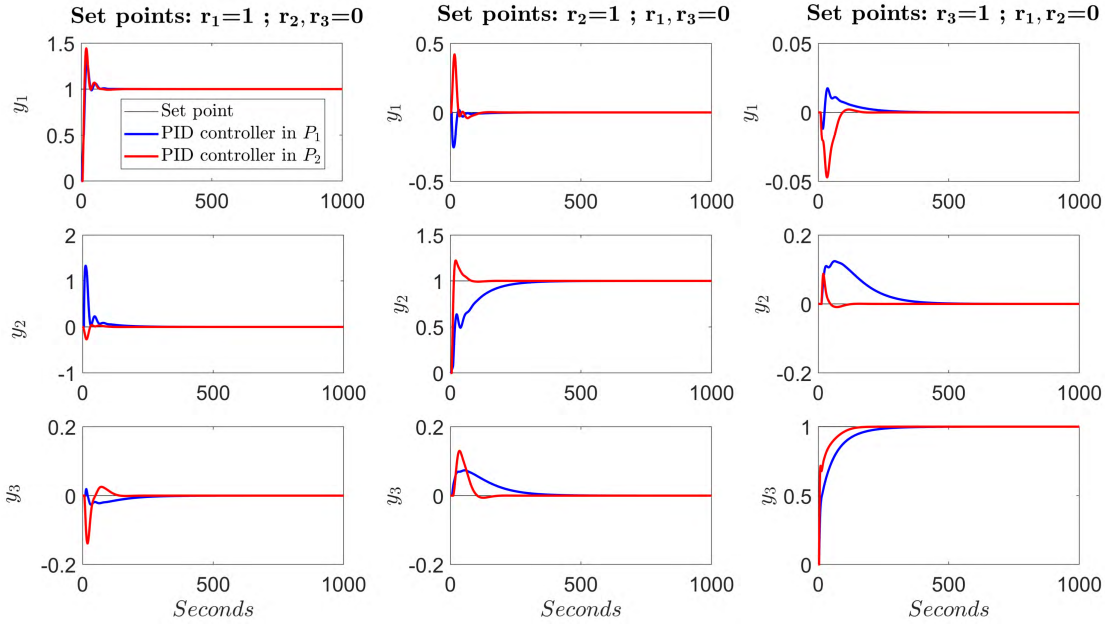

FIGURE 18. Responses of the PID controllers selected in the Pareto fronts of the second example.

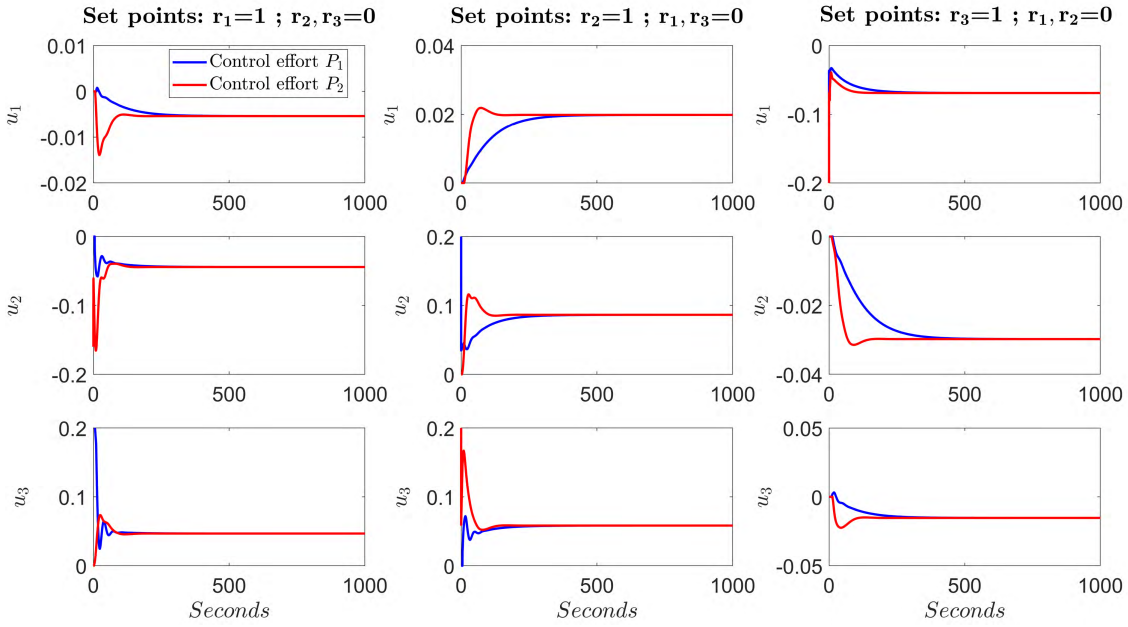

FIGURE 19. Control efforts of the PID controllers selected in the Pareto fronts of the second example.

$$J_\eta(\mathbf{x}^{ck}) = \int_0^{t_f} |e_\eta|\Big|_{r_1=1}^{r_2,r_3=0} dt + \int_0^{t_f} |e_\eta|\Big|_{r_2=1}^{r_1,r_3=0} dt + \int_0^{t_f} |e_\eta|\Big|_{r_3=1}^{r_1,r_2=0} dt \tag{82}$$

$$J_{\eta+3}(\mathbf{x}^{ck}) = \int_0^{t_f} \left|\frac{du_\eta}{dt}\right|\Big|_{r_1=1}^{r_2,r_3=0} dt + \int_0^{t_f} \left|\frac{du_\eta}{dt}\right|\Big|_{r_2=1}^{r_1,r_3=0} dt + \int_0^{t_f} \left|\frac{du_\eta}{dt}\right|\Big|_{r_3=1}^{r_1,r_2=0} dt \tag{83}$$

$$\eta = 1, 2 \text{ and } 3$$

$$t_f = 1000 \text{ seconds}$$

$$\underline{\mathbf{x}}^{ck} \le \mathbf{x}^{ck} \le \overline{\mathbf{x}}^{ck} \tag{84}$$

$$J_1(\mathbf{x}^{ck}) \le 400, J_2(\mathbf{x}^{ck}) \le 400, J_3(\mathbf{x}^{ck}) \le 300,$$
$$J_4(\mathbf{x}^{ck}) \le 1, J_5(\mathbf{x}^{ck}) \le 1, J_6(\mathbf{x}^{ck}) \le 0.5 \tag{85}$$

$$\mathbf{x}^{ck} = [K_1^{ck}, Ti_1^{ck}, Td_1^{ck}, K_2^{ck}, Ti_2^{ck}, Td_2^{ck}, \times K_3^{ck}, Ti_3^{ck}, Td_3^{ck}] \tag{86}$$

TABLE 13. Bounds of the decision vectors $\mathbf{x}^{c1}$ and $\mathbf{x}^{c2}$ for the second example.

Bounds of $\mathbf{x}^{ck}$									
$\mathbf{x}^{c1}$	K_1^{c1}	Ti_1^{c1}	Td_1^{c1}	K_2^{c1}	Ti_2^{c1}	Td_2^{c1}	K_3^{c1}	Ti_3^{c1}	Td_3^{c1}
$\underline{\mathbf{x}}^{c1}$	0.01	1	0.01	0.01	1	0.01	-1	1	0.01
$\overline{\mathbf{x}}^{c1}$	1	50	1	1	50	1	-0.01	50	1
$\mathbf{x}^{c2}$	K_1^{c2}	Ti_1^{c2}	Td_1^{c2}	K_2^{c2}	Ti_2^{c2}	Td_2^{c2}	K_3^{c2}	Ti_3^{c2}	Td_3^{c2}
$\underline{\mathbf{x}}^{c2}$	-1	1	0.01	0.01	1	0.01	-1	1	0.01
$\overline{\mathbf{x}}^{c2}$	-0.01	50	1	1	50	1	-0.01	50	1

TABLE 14. Controllers P_1 and P_2 selected in Fig. 17. The design objectives of each controller are compared and highlighted in bold.

Loop pairing LP_1		Loop pairing LP_2	
Parameters	P_1	*Parameters*	P_2
K_1^{c1}	0.2021	K_1^{c2}	-0.052
Ti_1^{c1}	17.34	Ti_1^{c2}	2.89
Td_1^{c1}	0.694	Td_1^{c2}	0.209
K_2^{c1}	0.035	K_2^{c2}	0.058
Ti_2^{c1}	24.71	Ti_2^{c2}	3.24
Td_2^{c1}	0.479	Td_2^{c2}	0.282
K_3^{c1}	-0.036	K_3^{c2}	-0.069
Ti_3^{c1}	21.37	Ti_3^{c2}	19.02
Td_3^{c1}	0.314	Td_3^{c2}	0.536
$J_1(\mathbf{x}^{c1})$	**20.88**	$J_1(\mathbf{x}^{c2})$	26.07
$J_2(\mathbf{x}^{c1})$	114.85	$J_2(\mathbf{x}^{c2})$	**23.11**
$J_3(\mathbf{x}^{c1})$	55.58	$J_3(\mathbf{x}^{c2})$	**13.31**
$J_4(\mathbf{x}^{c1})$	**0.122**	$J_4(\mathbf{x}^{c2})$	0.131
$J_5(\mathbf{x}^{c1})$	0.186	$J_5(\mathbf{x}^{c2})$	**0.053**
$J_6(\mathbf{x}^{c1})$	**0.187**	$J_6(\mathbf{x}^{c2})$	0.199

The bounds of $\mathbf{x}^{ck}$ are shown in Table 13.

Fig. 17 shows the Pareto fronts of each pairing, LP_1 and LP_2. The first thing that stands out is that it is possible, in both loop pairings, to find controllers with good performance for any of the objectives independently. The greatest difference can be seen in J_1, where LP_1 can achieve a better performance than LP_2. The solution P_1 is chosen for LP_1 and it is observed that there is a conflict between the objectives J_1, J_2, J_3, i.e. improving the performance of the output y_1 has the effect of worsening the performance of y_2 and y_3. This does not happen with LP_2, where it is feasible to find a trade-off zone (green solutions: $J_1 < 30.5, J_2 < 33.2, J_3 < 23.8$), where there are solutions with a satisfactory performance for the three system outputs. The solution P_2 was chosen in this area and it is observed that this solution does not present a conflict between the objectives J_1, J_2, J_3 but between these and the control efforts (especially with u_3). With respect to the control efforts (J_4, J_5, J_6), it is observed in the Pareto fronts that both controllers have very close efforts for the inputs u_1 and u_3, but for the input u_2 the effort of the controller in P_2 is much less than that of P_1.

Table 14 shows the performance of the outputs and the control efforts for the solutions P_1 and P_2 selected on each Pareto front. Fig. 18 shows the system outputs. It can be seen that the controller P_1 is slightly better than P_2 to control the output y_1, but the controller P_2 represents a noticeable improvement over P_1 to control the outputs y_2 and y_3. Fig. 19 shows the control efforts of each controller, P_1 and P_2.

VI. CONCLUSIONS

In this paper a new method to select input-output pairings in MIMO systems using a multi-objective optimization approach has been presented. In this approach, the control structure, the design objectives of the MOP, the optimal adjustment of the controller parameters, and the designer's preferences have an important role in the selection of a certain input-output pairing.

The method proposes a multivariable control structure as an alternative or design concept. Each design concept to be compared has a type of control and an associated loop pairing. For each design concept an MOP is proposed, and the Pareto front is obtained with the optimal settings of the controller parameters. This enables an m -dimensional analysis of the benefits of the possible types of loop pairings. In this way, a detailed analysis of the performance of the MIMO systems can be made, as well as the conflicts that occur when choosing a certain input-output pairings.

The method is applied to 2×2 and 3×3 systems. For the 2×2 system, RGA clearly proposes a diagonal pairing, while DRGA prefers an off-diagonal pairing. To show how the designer's preferences can influence when choosing one or another loop pairing, and show the proposed method, several scenarios are analyzed. The ISE, ISU, IAE, IADU indexes are proposed as control performance indicators. In the first example, the designer initially gives the same relative importance to the ISE and ISU, for which they are added in a single objective to be minimized. In this case, the off-diagonal concept is better than the diagonal concept. The designer makes a decision *a priori* and obtains a single optimal solution for each loop pairing. From this initial example, the first scenario is proposed by disaggregating the MOP into two design objectives. This scenario reveals that the off-diagonal design concept does not dominate the diagonal concept completely, since it is only preferable in a certain area of interest. In the second scenario, errors in the outputs and control efforts are analyzed partially independently (without mixing), and an MOP with four objectives is proposed. The analysis of the Pareto fronts of each design concept reveals that the diagonal concept has better characteristics than the off-diagonal concept. In fact, the off-diagonal concept would be eligible only if a designer gives greater importance to the objective J_2 (ISE associated with the output y_2). This shows that the designer in the initial example selected this preference without awareness, because when mixing ISE and ISU of both outputs and inputs, this phenomenon was hidden.

In the third scenario, an MOP with eight design objectives is proposed. In this scenario, the errors of each output (ISE) and the control efforts (ISU) are analyzed independently. The complexity of the analysis of the trade-off between objectives increased, but there is a much greater level of detail for a designer to take an optimal solution for the MOP. To reduce the size of the MOP and decrease the complexity of the decision-making stage, a designer may decide to combine the design objectives that are not in conflict.

Later, because the control actions are very oscillatory in the previous scenarios, it was decided to change the design objectives of the MOP. This produced a radical change in the system responses, and now the diagonal design concept was widely preferred over the off-diagonal concept. In this way, it was revealed how the designer's preferences through the choice of MOP objectives, can condition the choice of input-output pairing.

The application of the MO method to the 3×3 system shows again that according to the preferences of the designer LP_1 or LP_2 would be preferred. Contrary to what is manifested in [15], it is observed that LP_2 is not clearly better than LP_1. With a proper parameter setting of the controllers of LP_1 it is possible to control the system satisfactorily. The pairing LP_2 has a zone with satisfactory solutions for the three system outputs, while the pairing LP_1 has a conflict between its outputs, that is to say, improving one implies worsening the others. If the preference of the designer is to obtain a good control for all the outputs (accepting their corresponding increase in the control effort), then the pairing LP_2 would be the one chosen.

An advantage of the presented methodology is that it enables analyzing the dynamics of a closed loop system for selecting one loop pairing or another *a posteriori*. The selection of an input-output pairing and the conditions of the process (plant) are based on the designer's preferences (with a level of complexity selectable by the designer).

Future work will focus on expanding the proposed approach for nonlinear systems, and uncertain multivariable systems. It would also be interesting to analyze systems with restrictions on the outputs, or in which a certain loop pairing must go out of line for maintenance.

It is predictable that the number of parameters and objectives to be optimized will require improving the computational cost of the optimization algorithms and the visualization tools for the Pareto fronts.

APPENDIX A
ANALYSIS OF THE COMPUTATIONAL COST OF THE PROPOSED LOOP PAIRING METHOD

First of all, it must be made clear that the computational cost of the proposed methodology is difficult to generalize, since it depends on many factors. In general, it is higher than the computational cost of many of the classic loop pairing methods. However, it should be noted that the methodology takes into account the preferences of the designer, the type of controllers used and the tuning of their parameters. These considerations are decisive in the loop pairing and they cannot be ignored if a pairing adjusted to the needs of the designer is desired. Therefore, it would not be entirely fair to compare computationally the proposed methodology with classical methodologies, since the cost of loop pairing cannot be separated from the cost of tuning the control structure. Nevertheless, this section provides a reflection on the computational cost that would have to be assumed when applying the proposed methodology.

The computational cost (CC) of the proposed loop pairing method depends mainly on the number of MOPs that are proposed and the computational cost of each of them, see (87).

$$CC = \sum_{k=1}^{w} CC(MOP_{\mathbf{c}_k}) \tag{87}$$

The number of MOPs is equal to the number of design concepts $\mathbf{c}_k$ to analyze. As can be seen in (11) a design concept consists of a given loop pairing and the controllers associated with each control loop. The number of loop pairings to be studied will be at least two, but in a system $n \times n$ there can exist until $n!$ possible pairings.

The computational cost of a MOP depends on three factors: 1) the number of solutions evaluated in the optimization process (η_p), 2) the cost of calculating the chosen design objectives CC_J (shown in (16)) and 3) the cost of the MO algorithm itself (CC_{MO}).

$$CC(MOP_{\mathbf{c}_k}) = \eta_p CC_J + CC_{MO} \tag{88}$$

Normally, $\eta_p CC_J >>> CC_{MO}$, because CC_J has associated simulations (n_{simul}) of the controlled system that must be performed to calculate the objectives (which usually measure performance and control efforts). On the other hand, η_p depends on the number of evaluations of the objective function required by the optimization algorithm used. It should be noted that the computational cost of the optimization can vary considerably if, for example, the execution is parallelized. It is not the objective of this work to discuss the optimization algorithm used, since the methodological proposal is independent of the selected algorithm.

As can be concluded from what has been said so far, there are a lot of variables that make it difficult to determine the computational cost. In order to quantify it, the following assumptions will be made:

1) To consider CC_{MO} negligible.
2) Given a specific loop pairing problem, all concepts will have the same computational cost.
3) $CC_J = n_{simul} \cdot CC_{simul}$, considering that, given a particular problem, the cost of a simulation is always the same.

Therefore:

$$CC \approx w \cdot \eta_p \cdot n_{simul} \cdot CC_{simul} \tag{89}$$

For example, if the designers only want to analyze one type of controller for each pairing loop (among the n_{loops} that they want to study) and the number of simulations $n_{simul} = n$, then the computational cost will be:

$$CC \approx n_{loops} \cdot \eta_p \cdot n \cdot CC_{simul}, \tag{90}$$

with $n_{loops} \in [2 \ldots n!]$.

The computational cost in the examples 1 and 2 which have been proposed in this article was evaluated on a hardware platform with an Intel(R) Core(TM) i7-7700HQ processor (2.80 GHz, 16 GB RAM) and with MATLAB R2017b. In both examples, $\eta_p = 8000$ solutions were evaluated and

two design concepts were analyzed, one for each pairing ($n_{loops} = 2$). The number of simulations was $n_{simul} = n = 2$ for example 1 and $n_{simul} = n = 3$ for example 2. For example 1 the second scenario was chosen. A computational cost of $13.256 \cdot 10^3$ seconds was measured. For example 2 the computational cost was $26.146 \cdot 10^3$ seconds.

REFERENCES

[1] L. Bakule, "Decentralized control: An overview," *Annu. Rev. Control*, vol. 32, no. 1, pp. 87–98, Apr. 2008.

[2] D. D. Šiljak, "Decentralized control and computations: Status and prospects," *Annu. Rev. Control*, vol. 20, pp. 131–141, Jan. 1996.

[3] V. Kariwala, J. F. Forbes, and E. S. Meadows, "Integrity of systems under decentralized integral control," *Automatica*, vol. 41, no. 9, pp. 1575–1581, Sep. 2005.

[4] A. Khaki-Sedigh and B. Moaveni, *Control Configuration Selection for Multivariable Plants*, vol. 391. Berlin, Germany: Springer-Verlag, 2009.

[5] P. Li, X. Yang, and Y. A. W. Shardt, "Simultaneous robust, decoupled output feedback control for multivariate industrial systems," *IEEE Access*, vol. 6, pp. 6777–6782, 2018.

[6] K. Peng, D. Fan, F. Yang, L. Gou, and W. Lv, "A frequency domain decoupling method and multivariable controller design for turbofan engines," *IEEE Access*, vol. 5, pp. 27757–27766, 2017.

[7] A. Agrawal, O. Harib, A. Hereid, S. Finet, M. Masselin, L. Praly, A. D. Ames, K. Sreenath, and J. W. Grizzle, "First steps towards translating HZD control of bipedal robots to decentralized control of exoskeletons," *IEEE Access*, vol. 5, pp. 9919–9934, 2017.

[8] M. Van de Wal and B. de Jager, "A review of methods for input/output selection," *Automatica*, vol. 37, no. 4, pp. 487–510, Apr. 2001.

[9] E. Bristol, "On a new measure of interaction for multivariable process control," *IEEE Trans. Autom. Control*, vol. AC-11, no. 1, pp. 133–134, Jun. 1966.

[10] J.-W. Chang and C.-C. Yu, "The relative gain for non-square multivariable systems," *Chem. Eng. Sci.*, vol. 45, no. 5, pp. 1309–1323, 1990.

[11] T. M. Avoy, Y. Arkun, R. Chen, D. Robinson, and P. Schnelle, "A new approach to defining a dynamic relative gain," *Control Eng. Pract.*, vol. 11, no. 8, pp. 907–914, Aug. 2003.

[12] K. E. Häeggblom, "Partial relative gain: A new tool for control structure selection," in *Proc. AIChE Annu. Meeting, Citeseer*, Nov. 1997, pp. 16–21.

[13] Q. Xiong, W.-J. Cai, M.-J. He, and M. He, "Decentralized control system design for multivariable processes-a novel method based on effective relative gain array," *Ind. Eng. Chem. Res.*, vol. 45, no. 8, pp. 2769–2776, Mar. 2006.

[14] A. Balestrino, E. Crisostomi, A. Landi, and A. Menicagli, "ARGA loop pairing criteria for multivariable systems," in *Proc. 47th IEEE Conf. Decis. Control*, Dec. 2008, pp. 5668–5673.

[15] M.-J. He, W.-J. Cai, W. Ni, and L.-H. Xie, "RNGA based control system configuration for multivariable processes," *J. Process Control*, vol. 19, no. 6, pp. 1036–1042, Jun. 2009.

[16] L. Lenis, M. A. Giraldo, and J. J. Espinosa, "Methodology for the decomposition of dynamical systems based on input-output pairing techniques," in *Proc. IEEE 3rd Colombian Conf. Autom. Control (CCAC)*, Oct. 2017, pp. 1–7.

[17] A. Ahmadi and M. Aldeen, "New input-output pairing based on eigenvalue contribution measures," in *Proc. 9th Asian Control Conf. (ASCC)*, Jun. 2013, pp. 1–6.

[18] Q. Xiong, W.-J. Cai, and M.-J. He, "A practical loop pairing criterion for multivariable processes," *J. Process Control*, vol. 15, no. 7, pp. 741–747, Oct. 2005.

[19] A. S. Potts, L. C. Massaro, and C. Garcia, "Detection of decoupled input/output pairs in multivariable systems," *ISA Trans.*, vol. 55, pp. 195–207, Mar. 2015.

[20] T. N. L. Vu and M. Lee, "Independent design of multi-loop PI/PID controllers for interacting multivariable processes," *J. Process Control*, vol. 20, no. 8, pp. 922–933, Sep. 2010.

[21] S. Mollov, R. Babuska, and H. Verbruggen, "Analysis of interactions in MIMO Takagi-Sugeno fuzzy models," in *Proc. 10th IEEE Int. Conf. Fuzzy Syst.*, Dec. 2001, pp. 769–773.

[22] C. Xu and Y. C. Shin, "Interaction analysis for MIMO nonlinear systems based on a fuzzy basis function network model," *Fuzzy Sets Syst.*, vol. 158, no. 18, pp. 2013–2025, Sep. 2007.

[23] J. Bao, K. H. Chan, W. Z. Zhang, and P. L. Lee, "An experimental pairing method for multi-loop control based on passivity," *J. Process Control*, vol. 17, no. 10, pp. 787–798, Dec. 2007.

[24] W. Z. Zhang, J. Bao, and P. L. Lee, "Decentralized unconditional stability conditions based on the passivity theorem for multi-loop control systems," *Ind. Eng. Chem. Res.*, vol. 41, no. 6, pp. 1569–1578, Feb. 2002.

[25] V. Kariwala and Y. Cao, "Branch and bound method for multiobjective pairing selection," *Automatica*, vol. 46, no. 5, pp. 932–936, May 2010.

[26] J. M. Herrero, G. Reynoso-Meza, C. Ramos, and X. Blasco, "Considerations on loop pairing in MIMO processes. A multi-criteria analysis," *IFAC-PapersOnLine*, vol. 50, no. 1, pp. 4454–4459, Jul. 2017.

[27] M. G. Villarreal-Cervantes, A. Rodriguez-Molina, C. V. Garcia-Mendoza, O. Penaloza-Mejia, and G. Sepulveda-Cervantes, "Multi-objective on-line optimization approach for the DC motor controller tuning using differential evolution," *IEEE Access*, vol. 5, pp. 20393–20407, 2017.

[28] G. R. Meza, X. Blasco, J. Sanchis, and J. M. Herrero, *Controller Tuning With Evolutionary Multiobjective Optimization: A Holistic Multiobjective Optimization Design Procedure*, vol. 85. Cham, Switzerland: Springer, 2016.

[29] G. Reynoso-Meza, S. Garcia-Nieto, J. Sanchis, and F. X. Blasco, "Controller tuning by means of multi-objective optimization algorithms: A global tuning framework," *IEEE Trans. Control Syst. Technol.*, vol. 21, no. 2, pp. 445–458, Mar. 2013.

[30] X. Zhou, J. Zhou, C. Yang, and W. Gui, "Set-point tracking and multi-objective optimization-based PID control for the goethite process," *IEEE Access*, vol. 6, pp. 36683–36698, 2018.

[31] B. Srinivas, P. R. Kumar, B. Sreenivasulu, and K. V. Ramesh, "An efficient method to design a series cascade controller using multi-objective optimization," in *Proc. Int. Conf. Electron., Commun. Aerosp. Technol. (ICECA)*, Apr. 2017, pp. 218–224.

[32] J. M. Herrero and J. M. Martínez, J. Sanchis, X. Blasco, "Well-distributed Pareto front by using the e-MOGA evolutionary algorithm," in *Proc. 9th Int. Work Conf. Artif. Neural Netw.*. Berlin, Germany: Springer-Verlag, 2007, pp. 292–299.

[33] M. Behzadian, S. K. Otaghsara, M. Yazdani, and J. Ignatius, "A state-of the-art survey of TOPSIS applications," *Expert Syst. Appl.*, vol. 39, no. 17, pp. 13051–13069, Dec. 2012.

[34] J. Zhu and K. W. Hipel, "Multiple stages grey target decision making method with incomplete weight based on multi-granularity linguistic label," *Inf. Sci.*, vol. 212, pp. 15–32, Dec. 2012.

[35] P. P. Bonissone, R. Subbu, and J. Lizzi, "Multicriteria decision making (MCDM): A framework for research and applications," *IEEE Comput. Intell. Mag.*, vol. 4, no. 3, pp. 48–61, Aug. 2009.

[36] A. V. Lotov and K. Miettinen, "Visualizing the Pareto frontier," in *Multiobjective Optimization* (Lecture Notes in Computer Science), vol. 5252. Berlin, Germany: Springer, 2008, pp. 213–243.

[37] A. Inselberg, "The plane with parallel coordinates," *Vis. Comput.*, vol. 1, no. 2, pp. 69–91, Aug. 1985.

[38] A. Inselberg, "Parallel coordinates: Visualization, exploration and classification of high-dimensional data," in *Handbook of Data Visualization* (Springer Handbooks of Computational Statistics). Berlin, Germany: Springer, 2008, pp. 643–680.

[39] X. Blasco, J. M. Herrero, J. Sanchis, and M. Martínez, "A new graphical visualization of *n*-dimensional Pareto front for decision-making in multiobjective optimization," *Inf. Sci.*, vol. 178, no. 20, pp. 3908–3924, Oct. 2008.

[40] X. Blasco, J. M. Herrero, G. Reynoso-Meza, and M. A. M. Iranzo, "Interactive tool for analyzing multiobjective optimization results with level diagrams," in *Proc. Genetic Evol. Comput. Conf. Companion (GECCO)*, vol. 17, Jul. 2017, pp. 1689–1696.

[41] T. Tušar and B. Filipič, "Visualization of Pareto front approximations in evolutionary multiobjective optimization: A critical review and the prosection method," *IEEE Trans. Evol. Comput.*, vol. 19, no. 2, pp. 225–245, Apr. 2015.

[42] G. Reynoso-Meza, X. Blasco, J. Sanchis, and J. M. Herrero, "Comparison of design concepts in multi-criteria decision-making using level diagrams," *Inf. Sci.*, vol. 221, pp. 124–141, Feb. 2013.

[43] R. T. Marler and J. S. Arora, "Survey of multi-objective optimization methods for engineering," *Struct. Multidisciplinary Optim.*, vol. 26, no. 6, pp. 369–395, Apr. 2004.
[44] K. Miettinen, J. Hakanen, and D. Podkopaev, "Interactive nonlinear multiobjective optimization methods," in *Multiple Criteria Decision Analysis* (International Series in Operations Research & Management Science). New York, NY, USA: Springer, 2016, pp. 927–976.
[45] C. A. Mattson and A. Messac, "Pareto frontier based concept selection under uncertainty, with visualization," *Optim. Eng.*, vol. 6, no. 1, pp. 85–115, Mar. 2005.

VíCTOR HUILCAPI received the B.S. degree in electronic engineering and the M.Sc. degree in automation and industrial control from the Escuela Superior Politécnica del Litoral (ESPOL), Guayaquil, Ecuador, in 2002 and 2015, respectively. He is currently pursuing the Ph.D. degree with the Universitat Politècnica de València (UPV), Spain. He is also an Associate Professor with the Universidad Politécnica Salesiana (UPS). His main research interests include the control and modeling of multivariable systems, process optimization, and multiobjective optimization techniques applied to engineering.

XAVIER BLASCO was born in Paris in 1966. He received the B.S. and Ph.D. degrees in industrial engineering from the Universitat Politècnica de València (UPV), Spain, in 1991 and 1999, respectively, and the Diploma degree in electrical engineering from the Ecole Supérieure d'Electricité (SUPELEC), France, in 1992. Since 1994, he has been with the Department of Systems Engineering and Automation, UPV, where he is currently a Full Professor. His research work is developed at the Institute of Automatic Control (ai2), UPV. His research interests include model-based predictive control, evolutionary optimization, and multi-objective optimization applied to engineering, as well as dynamic modeling and process control.

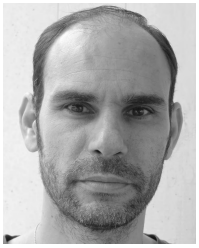

JUAN MANUEL HERRERO received the B.S. and Ph.D. degrees in control systems engineering from the Universitat Politècnica de València (UPV), in 1999 and 2006, respectively, where he is currently an Associate Professor with the Department of Systems Engineering and Automation. His main research interests include multivariable predictive control, process optimization, and computational intelligence methods for control engineering.

GILBERTO REYNOSO-MEZA received the B.Sc. degree in mechanical engineering from the Tecnológico de Monterrey, Campus Querétaro, México, in 2001, and the Ph.D. degree in automation from the Universitat Politècnica de València, Spain. He is currently with the Industrial and Systems Engineering Graduate Program (PPGEPS), Pontifícia Universidade Católica do Paraná (PUCPR), Brazil, as an Associate Professor. His main research interests include computational intelligence methods for control engineering and design, multi-objective optimization, many-objectives optimization, multi-criteria decision-making, evolutionary algorithms, and machine learning.